



Desiccants enabling energy-efficient buildings: A review

Ramy H. Mohammed^a, Masoud Ahmadi^b, Hongbin Ma^a, Sajjad Bigham^{b,*}

^a Multiphysics Energy Research Center (MERC), College of Engineering, University of Missouri-Columbia, 65211, USA

^b Department of Mechanical and Aerospace Engineering, North Carolina State University, Raleigh, NC, 27695-7910, USA



ARTICLE INFO

Keywords:

Desiccants
Air conditioning
Humidity pumps
Energy storage
Latent load
Buildings

ABSTRACT

Buildings account for about 39% of the total energy consumption in the United States. Developing highly energy-efficient and environmentally friendly systems that are either actively or passively integrated into buildings plays a crucial role in decarbonizing the building sector. Among various technologies, desiccant-based energy systems have received particular attention in recent years due to their unique advantages, such as being thermally driven using low-grade waste or solar energies and being reliable over a wide range of operating ranges. Extensive research efforts have been exerted on desiccant-enabled technologies at both material and system levels aiming to increase their performance and achieve high technological readiness levels. The present review paper comprehensively discusses research works made at the system level. It overviews desiccant-based air conditioning systems, desiccant-based humidity pumps, desiccant-based thermal energy storage systems, and desiccant-based appliances. The study identifies challenges and opportunities to accelerate the commercialization of desiccant-enabled technologies. It is found that desiccant materials offer great promise to improve energy efficiency and functionality of future buildings through decoupling the latent and sensible cooling loads in air conditioning systems, humidity pumps integrated into building facades, and next-generation appliances. However, commercial viability and widespread acceptance of desiccant-based systems have been hampered by several major obstacles, including liquid and air flow mal-distribution and inferior thermo-physical properties of desiccant materials resulting in low ab/adsorption and regeneration rates and bulky/costly systems.

1. Introduction

The global primary energy consumption is expected to rise by a factor of 5.0 by 2040 compared to 1970 [1]. The world's carbon emission is also envisioned to increase by a factor of 22.0 by 2040 compared to 1900 [1]. In the United States, the total energy consumption by residential and commercial buildings almost accounted for 39% of the total energy consumption in 2021 if the electricity losses (including transmission and distribution) were included [2]. Moreover, total (direct and indirect) carbon emissions from buildings are projected to reach about 6 Gt in 2030 [3]. Therefore, development of energy-efficient technologies is crucial to lower carbon emissions and reduce the energy consumption of the building sector, thus addressing the Sustainable Development Goals (SDGs), including good health and well-being, affordable and clean energy, and climate action [4].

Controlling moisture content in buildings is indispensable for occupants' health [5]. Buildings with high moisture levels offer a more suitable environment for mold and mites to grow [6]. A low-humidity environment is also desirable for many industrial applications,

including pharmaceutical, semiconductor, and lithium battery fabrication sites. Moisture removal (dehumidification process) is usually achieved using a condensation process employing a cold surface with a temperature lower than the air dewpoint. This process is traditionally achieved using a standard vapor compression cycle whose evaporator operates at a low temperature, and hence the air temperature and humidity decrease through the condensation process. A low-temperature condensation-based dehumidification process makes the independent control of the air temperature and humidity a challenge. It also provides air at a very low temperature that is not suitable to be supplied directly to occupied zones. A post-heater is often utilized to adjust the supply air temperature to the comfort zone, leading to additional energy consumption, especially in hot and humid regions. Decoupling the dehumidification and cooling processes is found to be an energy-efficient technique to achieve indoor air quality and thermal comfort [7–11].

Desiccant materials, either solid or liquid, are hygroscopic media with a high affinity to ad/absorb water vapor molecules from the atmosphere [12]. Here, the mass transfer process is governed by the difference between the partial water vapor pressure of the air stream and the equilibrium water vapor pressure of the desiccant media [10]. Solid

* Corresponding author.

E-mail address: sbigham@ncsu.edu (S. Bigham).

List of abbreviations	
AB	Absorption
AD	Adsorption
CD	Clothes Dryers
COP	Coefficient of Performance
DCS	Desiccant Cooling System
DW	Desiccant Wheel
EC	Evaporative Cooling
FSP	Federal Sustainability Plan
HAMP	Heat And Moisture Transfer Panel
HVAC	Heating, Refrigeration, and Air Conditioning
LD	Liquid Desiccant
M-cycle	Maisotsenko Cycle
MOF	Metal-Organic Framework
PV	Photovoltaic
PVT	Photovoltaic/Thermal
RCPs	Radiating Cooling Panels
REC	Regenerative Evaporative Cooler
SDGs	Sustainable Development Goals
SSLC/H	Separate Sensible and Latent Cooling/Heating
STES	Sorption-Based Thermal Energy Storage
SW	Sensible Wheel
TE	Thermoelectric
TES	Thermal Energy Storage
VCC	Vapor Compression Cycle
VCHP	Vapor Compression Heat Pump

desiccant materials are nanoporous with high internal surface areas and pore volumes. Silica gel, zeolite, activated carbon, and metal-organic frameworks (MOFs) have been used in buildings to remove moisture and control indoor climate conditions. Liquid desiccant materials are aqueous salt solutions that could be manipulated for enhanced heat and mass transfer rates. Lithium chloride (LiCl), lithium bromide (LiBr), calcium chloride (CaCl₂), and glycol are typical liquid desiccants that have been employed. A comparison between these two desiccant media is listed in Table 1 [13].

Due to the high potential of employing desiccant materials in buildings, extensive research efforts have been exerted in this direction. Fig. 1 presents the cumulative number of publications on desiccant materials for buildings. The data is extracted from Scopus Database [14] by searching the “desiccant” and “buildings, room, space, or zone” words in the title, keywords, and abstract. The figure shows that the number of publications steadily increased over the last 22 years. The total number of publications reached 1326 in 2022, compared to 213 in 2000 (about a six-fold increase). This trend indicates that desiccant-based technologies are receiving growing attention due to their promise for modern buildings. Analysis of the published works indicated that liquid and solid desiccants have been used for building applications. Also, extensive research efforts have been exerted at the material and system level to advance this technology to high technology readiness levels. Fig. 2 shows the research directions in desiccant-based systems for building applications. As shown, the research at the material level has mainly focused on conventional adsorbents (such as silica gel and zeolite) and advanced adsorbents (such as metal-organic frameworks and composites). Research at the material level aims to synthesize adsorbents with high adsorption rates and capacities, such as metal-organic frameworks and tuned silica gels [15,16]. At the system level, research efforts involve separate sensible and latent cooling and

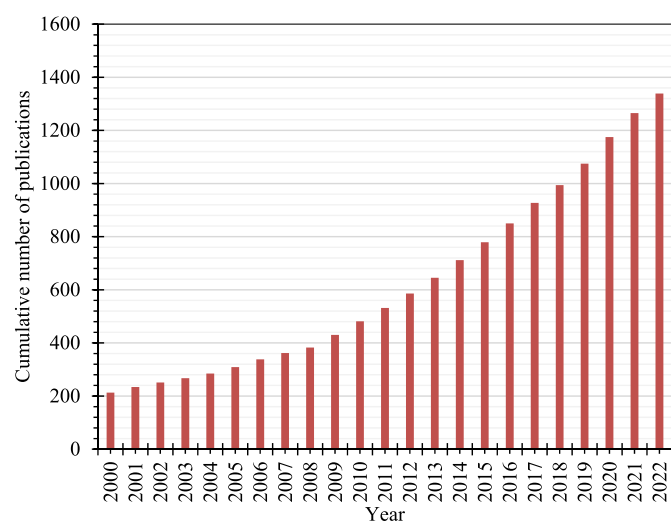


Fig. 1. Total number of publications on desiccant materials for buildings [14].

heating (SSLC/H) systems, humidity heat pumps, thermal energy storage (TES), and appliances. The main goal of these systems is to develop highly efficient equipment by enhancing the heat and mass transfer rates within the system [17–20]. For the SSLC/H systems, the desiccant-based system is explored to handle either sensible or latent loads for air conditioning applications. Humidity pumps aim to transfer humidity from a low to a high humid environment, thereby independently regulating the humidity level of living space. The desiccant system can be used as a thermal energy storage shedding or shifting thermal loads in future

Table 1
Comparison between the solid and liquid desiccants.

	Advantages	Disadvantages
Solid desiccants	<ul style="list-style-type: none"> High surface areas and pore volumes for the adsorption and regeneration processes. No liquid desiccant mal-distribution issue over solid surfaces. Several solid desiccants can be regenerated at low temperatures using waste and solar energies. Many solid desiccants are available at low costs. Many solid desiccants are compatible with eco-friendly adsorbates. 	<ul style="list-style-type: none"> Low thermal conductivity for rapid cooling during the adsorption or heating during the regeneration process. Low adsorption rate and capacity. Cyclic operation. Thermal and chemical stabilities are issues. No heat recovery between the adsorption and regeneration processes. Air mal-distribution is an issue. Bulky and heavy. Traditional liquid desiccants cause corrosion issues in contact with metals. Traditional liquid desiccants have crystallization issues during the desorption process. Limited performance in low humid climates. Mal-distribution of liquid desiccants. High initial costs.
Liquid desiccants	<ul style="list-style-type: none"> Ability to be regenerated at low temperatures using waste and solar energies. Enable solution heat recovery between absorption and desorption processes for higher energy efficiencies. Continuous operation. Many liquid desiccants are compatible with eco-friendly adsorbates. 	

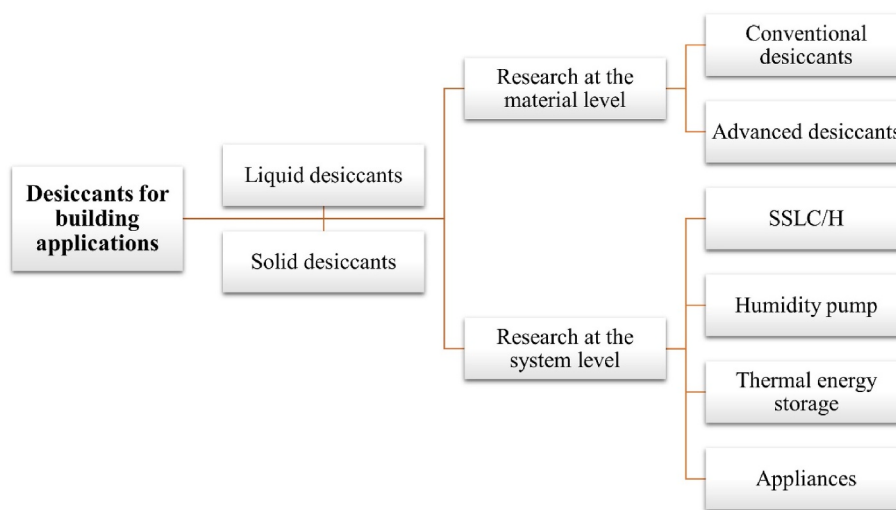


Fig. 2. Research directions in desiccant-based technologies for buildings.

sustainable buildings. Analysis of the published papers at the system level shows that the desiccant technology has been adapted as air conditioning units, humidity control devices, thermal energy storage systems, and appliances. It has been highlighted that desiccant-based systems can save energy in buildings. However, they are still at a low technological readiness level due to many challenges, such as low adsorption/desorption rate of materials and inefficient system designs. In the last few years, several review papers related to the potential applications of adsorption technology in buildings have been published. Each review paper discusses a specific application or technology. For instance, Tian et al. [1] reviewed the potential of using desiccant wheels to handle the latent heat loads in buildings. Guan et al. [21] discussed the liquid desiccant systems at the material and component levels. They presented the performance of various materials and systems. A similar study was presented by Salikandi et al. [22] where mixtures of liquid desiccants were reviewed. Shamim et al. [23] reviewed solid desiccant dehumidifier-based air conditioning systems with a focus on porous materials and their potential for achieving net zero carbon emissions in buildings.

The above literature review revealed that there is no review paper in the open literature that discusses desiccant-based technologies at the system level, particularly in Heating, Refrigeration, and Air Conditioning (HVAC) systems, building facades, and future appliances. Therefore, the current review article presents a comprehensive overview of the applications of desiccants for improving the energy efficiency and functionalities of future buildings. It covers the potential adaptation of desiccants for air conditioning systems, humidity control devices, thermal energy storage systems, and future appliances that promise energy saving in modern buildings. It also identifies research gaps and outlines recommendations to make further improvements in this field.

2. Desiccant-based air conditioning systems

The main component of a central air-cooling system is the cooling coil, whose surface temperature should be below the dewpoint of the outdoor air to be able to handle the latent cooling heat [24,25]. The typical relative humidity of the air leaving this cooling coil is 90–95% which is not suitable for entering a conditioned space due to its low temperature causing occupant discomfort from the cold draft, overcooling, and uneven temperature distribution, as well as the risk of creating cold spots near diffuser that leads to condensation and mold. Therefore, the relative humidity of air decreases by heating it sensibly. This approach is not energy-efficient due to the high energy consumption of the cooling and heating coils to adjust the thermodynamic

properties of supply air to the comfort zone. One of the proposed alternative approaches to address this problem is to separate sensible and latent cooling/heating (SSLC/H) loads in which the sensible and latent heat are handled separately, aiming to enhance the performance of the entire HVAC system [26]. The SSLC/H approach also allows for controlling the dry bulb temperature and humidity independently and dynamically. In the sensible cycle, the cooling coil could operate at higher temperatures, controlling the sensible load and leading to a higher coefficient of performance (COP) of the air conditioning unit (i.e., heat pump) [27]. The SSLC/H systems could be powered by renewable energy and alleviate the stress on the electricity grid. Therefore, it is a promising candidate to replace traditional HVAC systems [28].

Different cycles have been proposed to handle the sensible and latent load separately. The vapor compression cycle (VCC) is the dominant electrically driven technology. Desiccant-based systems, such as absorption (AB) and adsorption (AD) cycles, show great potential because they are thermally-driven systems with low carbon emissions. Depending on the temperature of the desiccant materials, the dry bulb temperature and moisture content of air can be changed, and hence thermal comfort of the conditioning space can be met.

2.1. Desiccants for sensible heat load management

Sorption systems have been applied to handle the sensible load in SSLC cycles. For example, Miyazaki et al. [29] carried out a theoretical study for the AD cycle having 3 beds of silica gel and two evaporators at two different temperatures. The evaporator with 7 °C handled the latent heat, while the 16 °C evaporator handled the sensible one. The system's COP was reported to be 0.65, which outperformed the traditional AD cycles by a factor of 1.7 at nominal conditions. Su and Zhang [30] coupled an AB cooling cycle to handle the sensible heat with a LiCl liquid desiccant cycle. The heat of condensation of the AB cycle was harvested to facilitate the desorption process of liquid desiccant. The AB evaporator operated at a higher value, and hence higher COP was achieved. It was reported that this coupled plant could have a primary energy efficiency (COP divided by energy conversion factor, which equals 90%) of 0.697 at an evaporator temperature of 18 °C and a condenser temperature of 46 °C. This efficiency is 34.97% higher than that of an AB unit. Habib et al. [31] proposed the system shown in Fig. 3, which has a desiccant dehumidification unit and an absorption (AB) chiller cycle. The AB cycle was coupled with a radiant cooling unit to produce cooled water. The state of outdoor air changes from state 1 to 3 by moving through the desiccant wheel (DW) and heating wheel (HW). Then, it experiences sensible cooling at constant moisture content when it passes

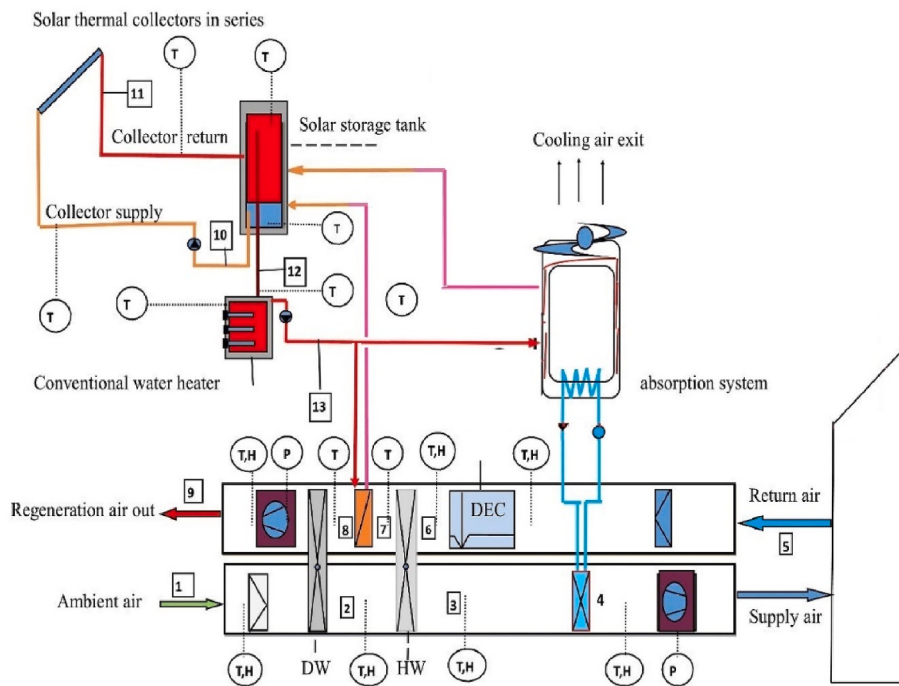


Fig. 3. A combination of AB cycle and desiccant wheel driven by solar energy [31].

over the coil of the absorption cycle. The AB cycle handles a sensible heat of 10.94 kW and the DW handles a latent heat of 4.44 kW. A mathematical model was built in TRNSYS software to investigate the system performance. The COP of the system was reported to be 1.52. While a COP of 0.52 was calculated for the AB cycle alone. The number of publications in this direction is found to be very limited due to the lower sensible cooling and heating capacities of sorption systems and lower COP compared to the vapor compression cycles. Therefore, it can be summarized that using solid desiccant materials for handling sensible heat in buildings is still at a low technological readiness level because of the low cooling power density of the available adsorbents at a sensible cooling temperature. In turn, solid desiccant materials have been extensively studied for removing the latent heat load, as discussed in the following sections.

2.2. Desiccants for latent heat load management

Due to the ability of sorbent materials to capture moisture from humid air, they have been widely used to remove latent heat from conditioned spaces [32,33]. Air conditioning units using desiccant materials can remove moisture from humid air using less energy than conventional units [34]. These units generally have a desiccant (dehumidification) wheel(s) (DW) employing solid materials, sensible heat wheels, and direct evaporative coolers [35]. The DW is a rotor that contains a solid desiccant material. While the wheel rotates, the desiccant undergoes adsorption and desorption processes. Hot air is usually utilized to regenerate the desiccant material. Therefore, DW has been widely used in air conditioning systems due to its simple design. In general, DW is coupled with another sensible heat technology for the entire system to handle the total load. The vapor compression cycle is usually coupled with DW, and this system is named a hybrid desiccant cooling system (DCS) [36]. Two evaluation parameters are considered to assess its performance: (i) the thermal COP, which is the system's cooling capacity divided by the thermal energy utilized for the desorption process, and (ii) the electrical COP, which is the system's cooling capacity divided by the electrical power used to drive the vapor compression vapor.

i Solid desiccant-based SSLC systems

According to the energy and exergy analyses carried out by Khosravi et al. [37], the DCS could save energy by 19.8% and reduce the running cost by 14.5% when compared to the traditional cycles. Jia et al. [38] studied a DCS in which the capacity of the vapor compression cycle was 6 kW at outdoor conditions of 30 °C and 55%. An electrical heater was utilized to regenerate the DW. In comparison with the traditional systems, their results showed that energy saving of about 37.5% could be achieved. Liu et al. [39] found that the DCS could maintain the room conditions at a certain level by adjusting the temperature of regeneration. An electrical COP of 3.044 was estimated from the numerical analysis when the outdoor humidity and temperature were 34.7% and 36 °C, respectively. Hürdoan et al. [40] constructed DCS with a heat recovery wheel to enhance indoor thermal comfort and reduce energy consumption. Silica gel was coated over the DW to take out the water vapor from the outdoor air. It was found that energy consumption mainly depends on the regeneration of heat. The electrical heater was used for the regeneration process and contributed 62% to the energy consumption at an average electrical COP of 1.35. Under outdoor conditions of 35 °C and 44% RH, Ling et al. [41] performed experiments on DCS. Compared to the traditional vapor compression cycles using CO₂, the tested system increased the electrical COP by 61%.

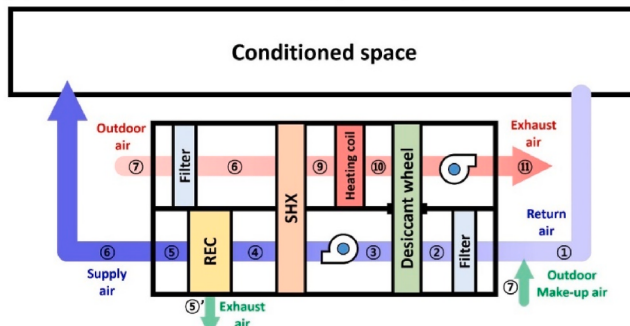
The experimental measurements carried out by Jiang et al. [42] showed the DCS using variable refrigerant flowrate produced an electrical COP in the range of 4.0–4.7 in July and August in Shanghai, China. Jani et al. [43] simulated in TRNSYS a zone equipped with DCS to handle a 1.8 kW cooling load in humid and hot conditions. The regeneration temperature and ambient humidity were the main parameters controlling the system's performance. An electrical COP of 5.5 was predicted at outdoor conditions of 30 °C, 59.6% RH, and 100 °C desorption temperature. The experimental measurements were carried out by the same research team [44] from March to October in Roorkee, India. It was revealed the capability of DW to handle 0.39 kW of latent heat. Under 32 °C outdoor temperature, an electrical COP of 2.0 was recorded. Lee et al. [45] reported that the DW integrated into mobile air conditioning could save energy by 26.3%. Lee et al. [46] modeled the thermodynamic behavior of three air conditioning systems. The first one

has a direct evaporative cooler and DW. The second one has an indirect evaporative cooler and DW. The third one is DCS. Although the capacity of the vapor compression cycle was much higher than that of an indirect evaporative cooler, its system provided higher COP when the ambient temperature was less than 35 °C. When this temperature increased, the COP of the third cycle (DCS) was more, owing to the higher capacity of the vapor compression cycle. The total COP of the third system was always the highest regardless of the ambient relative humidity. On the other hand, Choi and Choi [47] simulated the systems shown in Fig. 4, which are a combination between a regenerative evaporative cooler (REC), DW, and sensible wheel (SW). The evaporative was installed in the conditioned room to handle the sensible heat. In comparison with DW and the evaporative cooler system, the proposed system (Fig. 4b) had an electrical COP of 6.9 and reduced the energy by about 20–30%.

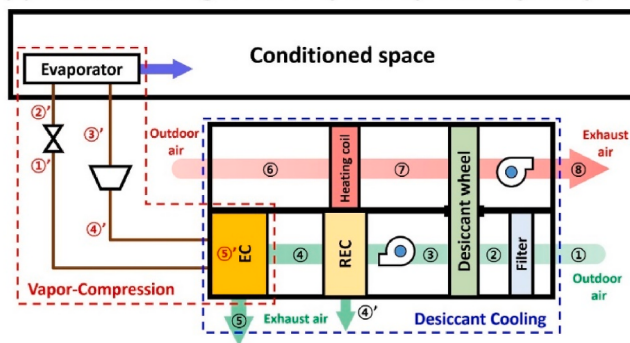
Instead of using the VCC and DW, researchers have coated the adsorbent materials over the heat exchangers of a vapor compression cycle. The operation of the cycle was modified to alternate between the condenser and evaporator to switch between the adsorption and desorption processes [48]. This approach allows the adsorption and desorption process to occur at almost constant temperatures. In this regard, Tu et al. [48] reported that this configuration could have an electrical COP of 7.0 while the system is more compact compared to the traditional DCS. Jani et al. [49] built an experimental test rig and made a theoretical analysis in TRNSYS for various arrangements of the coated vapor compression cycle. A room with an internal volume of 49 m³ and a total load of 1.76 with a sensible heat factor of 0.78 was tested in the summer conditions. The room conditions were set at 55% RH and 25 °C, while the outdoor temperature was 31 °C. Under these conditions, an electrical COP of 1.82 was estimated when the driving temperature was 70 °C. The electrical COP was 2.51 using a 50 °C regeneration temperature.

Owing to the merits of the Maisotsenko cycle (M-cycle), like its low cost and eco-friendly cycle, it has been coupled with a desiccant system for air conditioning purposes. Worek et al. [50] studied a system having

(a) Reference Desiccant Cooling System (RDCS)



(b) Desiccant Cooling assisted Vapor Compression System (DCVCS)

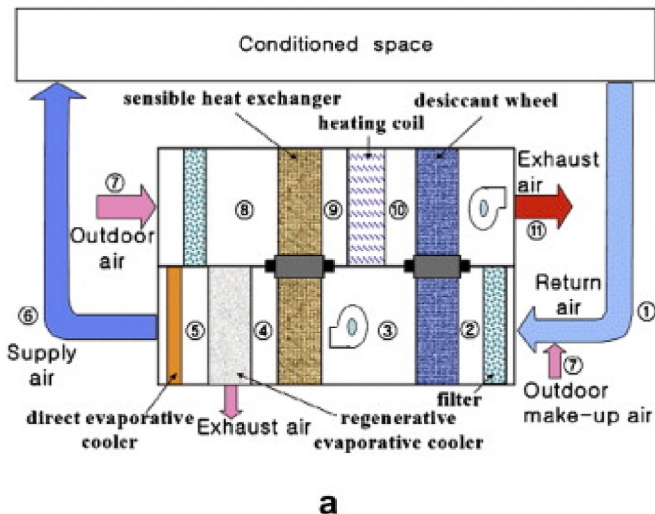


* SHX: Sensible Heat Exchanger REC: Regenerative Evaporative Cooler EC: Evaporative Condenser

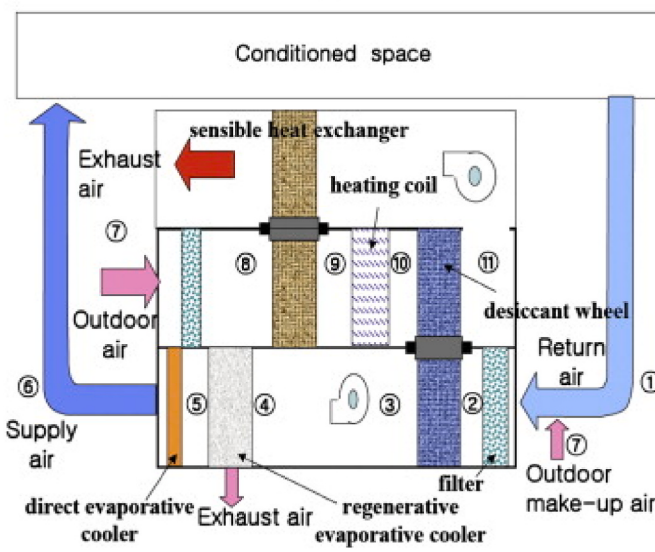
Fig. 4. Drawings of the systems investigated by Choi and Choi [47].

a DW and an indirect evaporative cooler (M-cycle). They confirmed the feasibility of using this system to replace the vapor compression cycle. In general, the energy and exergy performance (COP and exergy efficiency) of the system is inversely proportional to the regeneration temperature [51]. Pandelidis et al. [52] utilized silica gel DW with M-cycle to remove the latent and sensible heat from the conditioned room. A mathematical model was developed using the effectiveness-Number of Transfer Units (ε -NTU) to assess the feasibility of system. A temperature of 55–60 °C was used to regenerate the desiccant material. It was reported that the temperature of air supplied to the room increases monotonically with the increase in the outdoor humidity ratio and inlet flow rate. The regeneration temperature has the opposite effect on the supply air temperature. The system was able to provide air at 17.5 °C when the DW rotates with 8–10 turns per hour. Delfani and Karami [53] studied numerically three arrangements of air conditioning using DW, heat wheel, and M-cycle under various outdoor conditions. The regeneration process in the three systems was carried out using a solar air heater. It was found that a low regeneration temperature is needed during the hot climate. Thus, the studied systems performed well in hot and semi-humid climates. It was concluded that the maximum thermal COP of 0.728 could be achieved due to the low generation temperature applied in the DW.

Chung and Lee [54] studied the two desiccant systems shown in



a



b

Fig. 5. Schematics of the two air conditioning systems studied in Ref. [54].

Fig. 5 numerically using the analysis of variance (ANOVA). The systems have a sensible heat exchanger, heating coil, regenerative evaporative cooler, direct evaporative cooler, and desiccant wheel. The effect of design parameters on the performance of two SSLC arrangements was studied. Among various factors, the regeneration temperature was the dominant one shared by 31.9% and 23.9% in the COP of systems A and B, respectively. The operating and design conditions of system A were optimized, and a maximum COP of 1.286 was recorded. Caliskan et al. [55] built and field-tested system A proposed in Ref. [54] after removing the direct evaporative cooler. They carried out energy, exergy, and sustainability calculations. The air conditioning system was tested under the summer conditions of the Republic of Korea at a dry-bulb temperature of 35 °C and relative humidity of 39.75%. An electrical COP of 6.708, thermal COP of 0.769, electrically driven exergy COP of 0.463, and thermally driven exergy COP of 0.198 were estimated. It was highlighted that the solid DW has low exergy efficiency of 38.35% and, therefore, its design should be enhanced. Narayanan et al. [56] investigated DW with an enthalpy wheel, sensible wheel, and evaporative cooling. The proposed system was simulated under subtropical and tropical conditions. The system performed well under subtropical conditions during 93% of the running hours. The thermal COP changed from 0.21 to 0.36 for the tropical condition.

The energy consumed in the regeneration process of desiccant material is the main contribution to the total energy consumption and hence the COP of the entire system. Therefore, using solar energy to regenerate desiccant material has been proposed and widely applied in the literature. Beccali et al. [57] showed through their theoretical analysis the economic preference of DCS over the DW with an enthalpy wheel because it needed a smaller area of solar panels. Fong et al. [58] tested the feasibility of using solar energy to drive six configurations that have VCC, EC, and DW. In comparison with the standalone vapor compression cycles, the investigated systems have the potential to save energy by 35.2% with fewer carbon emissions. It was recommended to use an evacuated tube solar collector over the PV and PVT to drive the system because the capital and running costs were less. Moreover, the same research group studied DCS powered by an evacuated tube solar collector coupled with a water tank. Energy saving over the year was calculated to be 49.5% when the system was installed in a Chinese restaurant. Al-Alili et al. [59] concluded that using PVT solar collectors is twice more efficient as using PV panels under Abu Dhabi conditions. La et al. [60] experimentally and numerically calculated the COP of DCS driven by a solar collector. At highly humid conditions, the system was able to achieve an average electrical and thermal COP of 11.48 and 1.24, respectively. Angrisani et al. [61] performed energy and economic analysis in TRNSYS for DCS using silica gel as an adsorbent. They studied the effect of using various solar collectors at different angles under the climate conditions of Benevento and Milano cities in Italy. Their dynamic simulation concluded that a system using an evacuated tube solar collector performs better than others.

Saghafifar and Gadalla [62] studied numerically two cooling configurations having a solid desiccant system and M-cycle powered by PV/T panels under the humid climates of the UAE. When the solar system shared 32.2% and 36.5% of the regeneration process, the thermal COPs were 0.25 and 0.27, respectively. Chaudhary et al. [63] used solid DW coupled with an evacuated-tube solar collector to handle latent heat and M-cycle to handle sensible heat. The performance of the system was investigated experimentally under the climate conditions of Pakistan in May, June, and July. The air conditioning unit was able to provide a cooling power of 3.78 kW at a thermal COP of 0.91. Heidari et al. [64] modeled a system consisting of silica gel DW powered by an evacuated tube solar collector and evaporative cooler. Besides the cooling power, the proposed system could produce weekly potable water of 585 L. A portion of this water was used in the evaporative cooler. The studied unit achieved an average total COP of 1.53, which was about 27% more than the vapor compression cycle. The proposed unit consumed less electrical power by 60% and produced lower CO₂ emissions by 18.7%

compared to the vapor compression cycle.

Rayegan et al. [65] studied an air conditioning system that has DW integrated with a heat recovery wheel driven by solar energy and a direct evaporative cooler. They carried out dynamic and multi-objective optimization studies. The study aimed to minimize the regeneration temperature and maximize the thermal comfort index and solar contribution. A 95% thermal comfort index was achieved at an average electrical COP of 10.2. The economic study showed that the payback period of the system is 5.7 years. Liu et al. [66] simulated DCS where PV panels were used to drive the vapor compression cycle and solar collectors were utilized to facilitate the operating of silica gel DW. Electrical and thermal COPs of 6.25 and 2.75 were predicted, respectively, when the regeneration temperature was 55 °C. This result indicates the possibility of powering the system with low-grade energy. Song and Sobhani [67] studied two M-cycles. They proposed a solar PVT system integrated with phase change material to provide thermal energy and electricity to regenerate the desiccant. It was found that the best regeneration temperature is 70 °C at which the maximal thermal and exergetic COP of 0.415 and 1.3 were estimated, respectively. Saedpanah et al. [68] proposed an SSLC system that has a DW and an evaporative cooler, as presented in Fig. 6. Solar energy was used for the regeneration process. According to the mathematical model, the system could extract water from the ambient by 70% more than needed for the evaporative cooler. Although the system's COP was not calculated, the authors claimed that the system has a good potential to reduce carbon emissions and replace the vapor compression cycle.

Li et al. [69] experimentally tested a SSLC system driven by solar energy. It consisted of a two-stage DW and three evaporative coolers. The thermal and total COPs were measured to be 0.95 and 0.45, respectively, in humid and hot climates. Further investigation was performed for this system by Zeng et al. [70]. Transient simulation and optimization studies of the components were carried out using TRNSYS software. At a room temperature of 24.3 °C, an optimal COP of 0.85 and cooling energy of 2005 kWh could be achieved. Kousar et al. [71] experimentally carried out energy and economic analysis for various configurations of air conditioning systems using DW, heat wheel, and direct or indirect evaporative cooler. A solar unit was integrated into the system to produce hot water for the regeneration process. A system with an indirect evaporative cooler had the maximum thermal and electrical COPs of 1.85 and 3.9, respectively, at a cooling load of 5.26 kW using a regeneration temperature of 70 °C. Compared to the conventional system, the proposed one is more efficient from the economic point of view due to using solar energy to drive the system. Zhou et al. [72] used TRNSYS software to study the performance of DW regenerated by hot water from the solar system and M-cycle. The proposed system was not able to meet the thermal comfort requirements in tropical conditions. Under subtropical conditions, a 50% energy saving could be achieved.

Another approach proposed to regenerate the desiccant material is to use the heat rejected in the condenser of the vapor compression cycle. Among seven systems investigated by Ling et al. [73], they concluded that the energy consumption could be reduced when the heat rejected (heat of condensation) in the vapor compression cycle was recovered for the regeneration process in DW. Sheng et al. [74] made the same approach and achieved an electrical COP of 2.08 at an ambient moisture content of 20 g/kg. Luo et al. [75] built an experimental DCS in which the heat of condensation was harvested for the regeneration process. Experimental measurements revealed that using a solar system with a hot water tank reduces energy consumption by 10%. Nie et al. [76] analyzed DCS in which 100% return air was used, and two condensers were installed to use one of them to regenerate the silica gel. Under ambient conditions of 20.63 °C and 91.4% RH, the system produced an electrical COP of 3.47. The electrical COP reduced to 2.75 when the ambient conditions were 38.28 °C and 39.9% RH.

In summary, the performance of DCSs is relatively low due to the high regeneration energies and the low sorption rates of desiccant materials. Therefore, developing inexpensive and high-performance

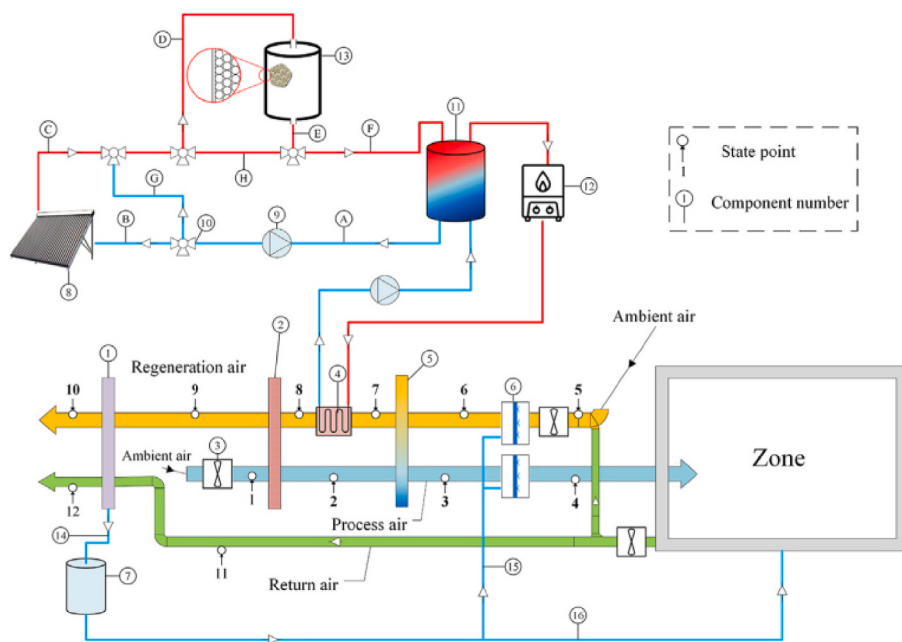


Fig. 6. A schematic diagram of SSLC cycle proposed in Ref. [68].

adsorbents is a barrier facing the market penetration of DCS technology. Also, the high required heat of the regeneration process makes these systems energy-intensive. Integrating the DCS with renewable energy resources, such as solar energy, for regeneration purposes has been proven to be a promising approach to cutting down the running cost due to using free heating energy. However, most studies have been performed at lab scales. Future works should focus on large-scale solid desiccant-based systems and assessment of their long-term operations.

ii Liquid desiccant-based SSLC systems

Liquid desiccant (LD) materials have a higher diffusion rate than solid desiccant materials. Therefore, using the LD technology has been adapted to handle the latent load. Mohammad et al. [77] concluded that the performance of an air conditioning cycle having LD depends on the

type of LD material. Also, they highlighted the advantage of utilizing solar energy in the regeneration process. Studak and Peterson [78] highlighted the high performance of systems using CaCl_2 because it is relatively cheap and has a good heat transfer coefficient. In turn, it is corrosive; hence, special materials should be used to construct the system. Kinsara et al. [79] studied a DCS using LD (LDCS). Their results indicated a reduction in energy consumption by 30% compared to the vapor compression cycle. Dai et al. [80] coupled an evaporative cooler to LDCS, and its total COP was calculated to be higher than that of the vapor compression cycle by 23%. Chen et al. [81] built and tested the experimental setup shown in Fig. 7. The system consists of an evaporative cooler for sensible heat and a CaCl_2 desiccant dehumidifier for latent heat. The measurements indicated the good potential of the proposed system in removing the sensible and latent heat. The moisture removal rate was enhanced by a factor of 2.0 when the relative humidity

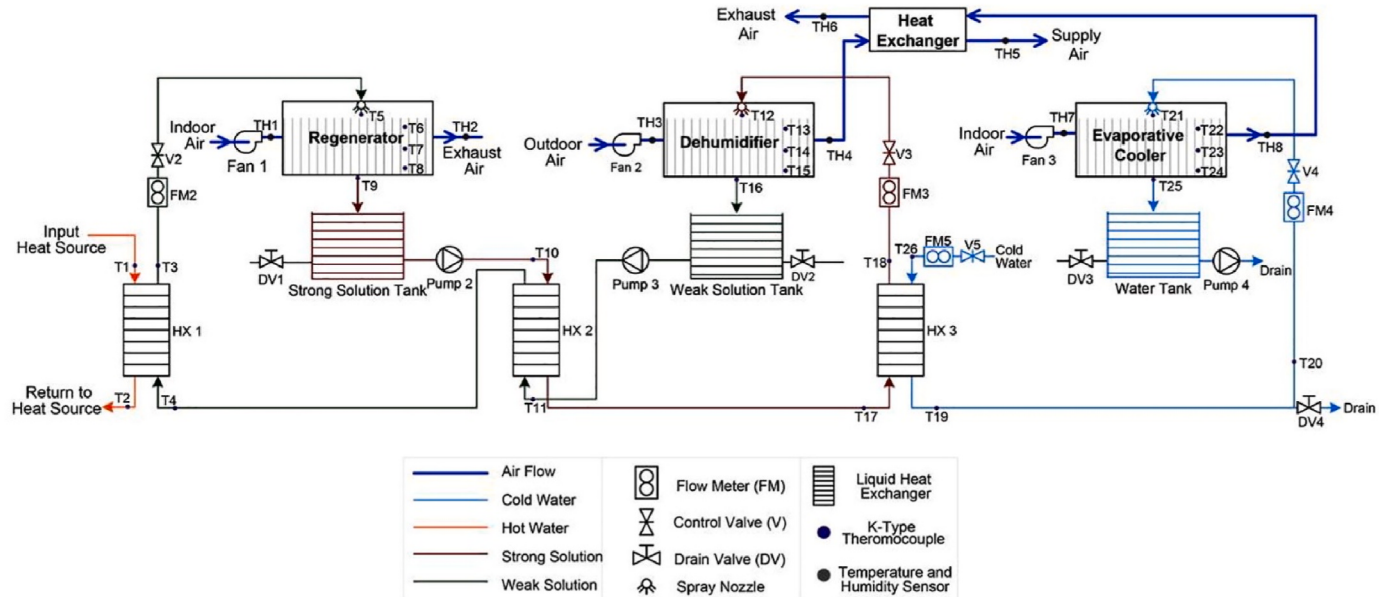


Fig. 7. A schematic of the air conditioning system studied in Ref. [81].

of air changed from 46% to 70%. Under steady-state conditions, the system's thermal COP was 0.70. Mansuriya et al. [82] did experimental tests on a lab-scale CaCl_2 LDGS presented in Fig. 8. In comparison with the vapor compression cycle, the tested system improved the electrical COP by about 27.5%. The same authors carried out energy and economic study to optimize the plant [83]. An enhancement of 68.4% in the electrical COP was achieved.

Khalil [84] experimentally tested LiCl LDGS in Egypt, where the temperature ranged from 20 to 30 °C and relative humidity changed from 35 to 45%. The plant handled a total load of 6.15 kW at an electrical COP of 3.8. A similar system was studied by Zhao et al. [85] for an office room in China, and an electrical COP of 4.0 was achieved. Simulation results reported by Bergero and Chiari [86,87] showed that LiCl LDGS could save energy by 60% at a low sensible heat factor. Zhang et al. [88,89] investigated the same system and found that a 30–40% increase in electrical COP could be achieved when the system is used for heating applications. Lee and Jeong [90] did measurements for LiCl LDGS installed in Korea. The system's COP was 2.26 for cooling and 2.51 for heating purposes. Yamaguchi et al. [91] investigated LiCl LDGS while the regenerator of the absorption cycle was integrated into the condenser of the vapor compression cycle, as drawn in Fig. 9. Also, the absorber was integrated into the evaporator. The electrical COP was 3.82 at a supply temperature of 22.2 °C. It was reported that the heat exchanger's effectiveness significantly affects the system's COP. Xie et al. [92] utilized the heat of condensation in the regeneration process of LDGS. The system produced the required load at an electrical COP of 9.7. In the LDGS studied by Liu et al. [93], the heat of condensation and evaporation were utilized in the regeneration and absorption process. The simulation results showed that the electrical COP could reach 6.68 when the solution heat exchanger was assumed to be highly efficient with an effectiveness of 1. Li et al. [94] constructed a LDGS using LiBr. Experimental measurements were carried out in a hospital in China, and the total COP was found to be 4.3 and 5.3 in the winter and summer seasons, respectively. He et al. [95] showed that the electrical COP of LiBr LDGS could be 7.08 when tested in the weather conditions of Zhengzhou in China. Also, a 26.7% reduction in energy consumption could be achieved compared to the vapor compression cycle. Guan et al. [96] highlighted the effect of fluid flow in heat exchangers on the performance of the LDGS. They concluded that the highest electrical COP of 7.4 is achieved using the counter-flow heat exchangers. The electrical COP dropped to 6.8 for parallel-flow configurations. Guan et al. [97] experimentally tested LDGS to cool a factory in Xiamen, China. The

annual saving in the electricity bill was calculated to be 23.3%, with an average electrical COP of 3.6. Song et al. [98] carried out a parametric study for LDGS and calculated the COP of the absorption cycle and vapor compression cycle to be 0.75 and 3.01, respectively. Ali et al. [99] built an experimental setup by integrating solid DW and gas absorption chiller, as drawn in Fig. 10. Silica gel and $\text{NH}_3\text{-H}_2\text{O}$ were used as sorbents for DW and absorption chiller, respectively. The COP was nearly the same as the double-effect absorption unit. Compared with another system having DW, heat recovery wheel, DEC, and heater, the tested system achieved a higher COP by 50–55% at a supply temperature of 15.2 °C.

Yong et al. [100] built a system from an indirect evaporator cooling and a vapor compression cycle with a liquid desiccant (LD) rotor using LiCl as an absorbent. The system was tested in the highly humid climate of Hong Kong. It was reported that the system's behavior is sensitive to the airflow rate and regeneration temperature. It could handle the required cooling loads with a maximum COP of 0.5 using a 100 °C regeneration temperature. The presence of the vapor compression cycle allowed the whole system to maintain higher COP at higher ambient temperatures. It was concluded that the proposed system is energy-saving and cost-effective under various operating modes. Abdel-Salam et al. [101] proposed a solar membrane LD air conditioning unit. Based on the heating source type (natural gas, electrical heat pump, solar system with natural gas boiler backup, and solar system with electrical heat pump backup and air streams arrangements, eight configurations were studied using TRNSYS software. It was concluded that using a solar system to regenerate the LD improves environmental and economic performance. Further enhancement was achieved when the natural gas boiler was utilized. These results confirmed the feasibility of using solar energy for the regeneration process of desiccant materials. Ma et al. [102] built a system by coupling DCS to two units of adsorption cycle using silica gel. Solar energy was utilized to drive the adsorption cycle, and the heat of condensation was harvested to regenerate the liquid desiccant. The vapor compression cycle and adsorption units were used to handle the sensible heat. The proposed system produced higher electrical COP than the traditional vapor compression cycles by 44.5%.

Desiccant has been integrated into evaporative coolers and used for air conditioning systems. The desiccant/evaporative cooler is cost-effective, environment-friendly, and a good alternative to conventional air conditioning systems. Rafique et al. [103] reviewed the potential of integrating desiccants in evaporative coolers. It was summarized that the evaporative cooler becomes more efficient when it

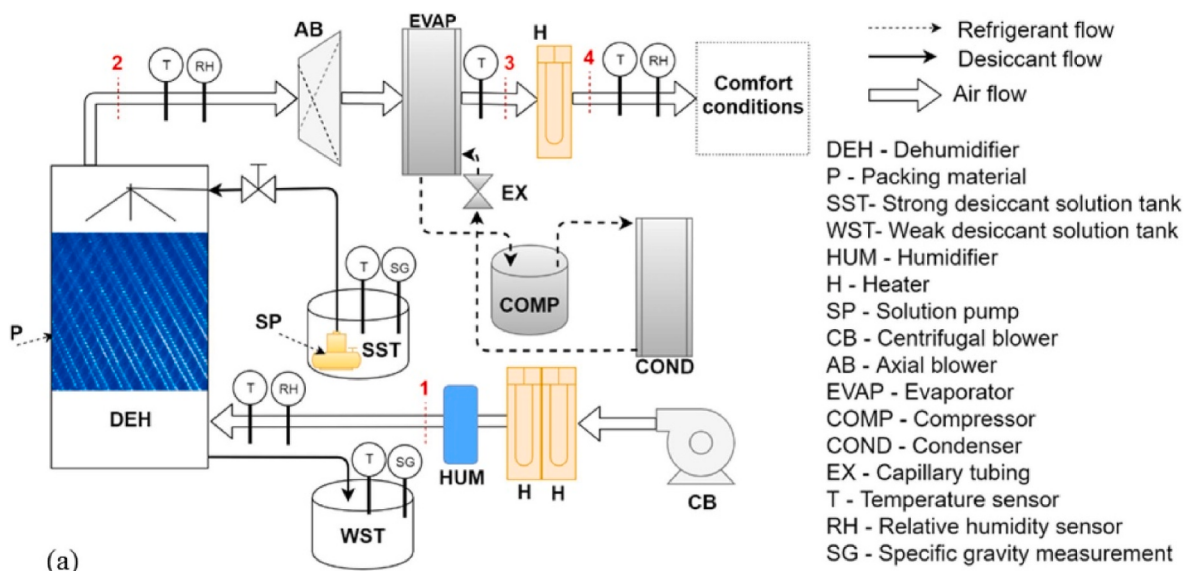


Fig. 8. A schematic of the air conditioning system studied in Ref. [82].

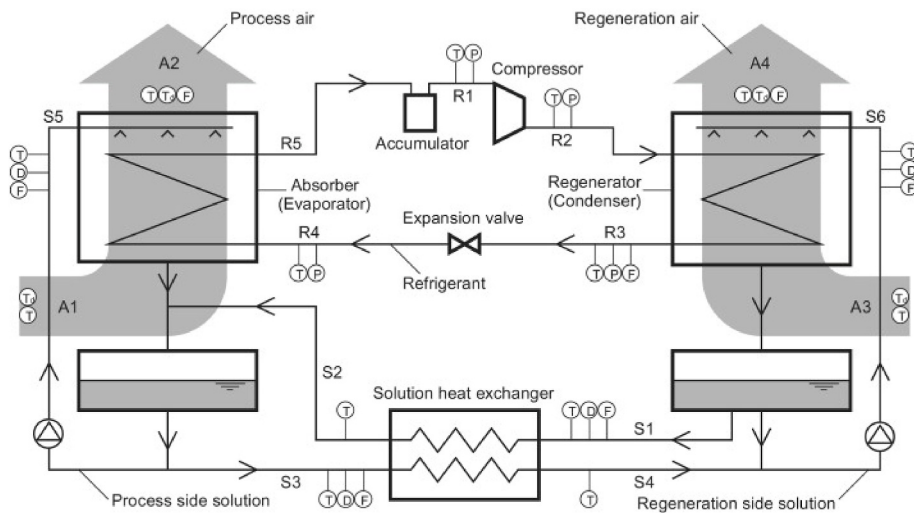


Fig. 9. A schematic diagram of the air conditioning system developed by Yamaguchi et al. [91].

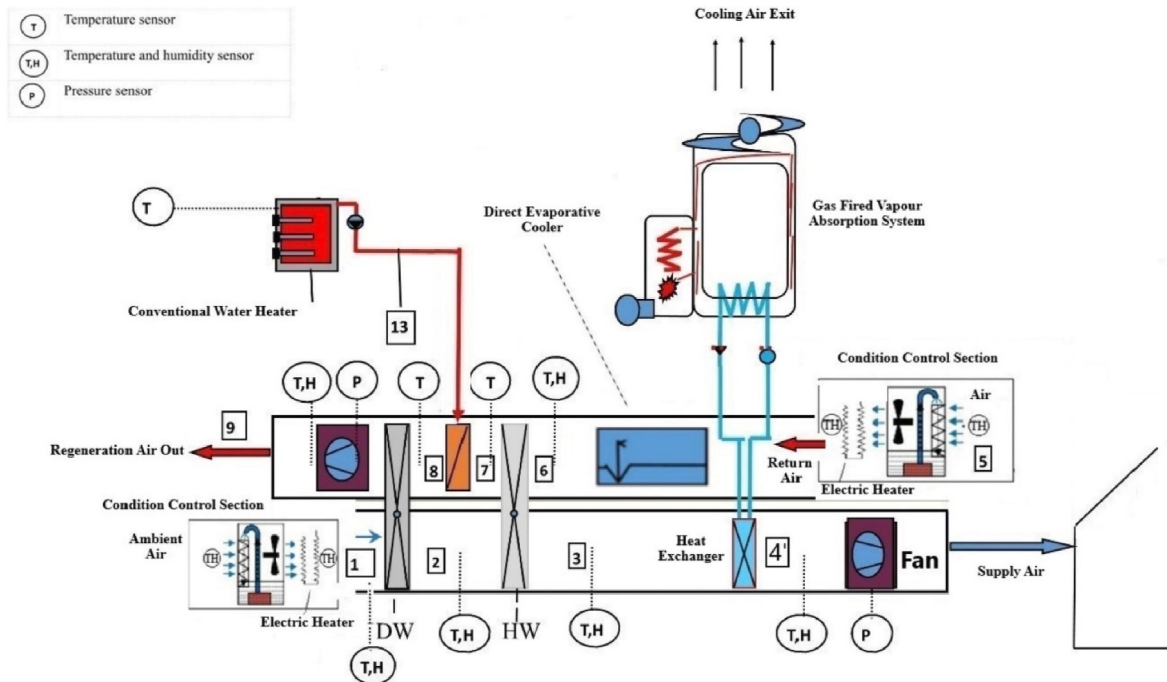


Fig. 10. A schematic diagram of the HVAC system investigated by Ali et al. [99].

is coupled with a desiccant dehumidifier. This integration is more suitable for hot and humid climatic zones. Solar energy or low-grade waste heat can be also used to facilitate the continuous operation of the desiccant/evaporative cooler systems. Buker and Riffat [104] reviewed the air conditioning systems using LD evaporative cooling units powered by solar energy. It was concluded that this integration can lead to 25–50% saving in the total energy consumption compared to the vapor compression cycle. Kim et al. [105] coupled LD into evaporative cooling. A heating coil and a sensible heat exchanger were added to the air conditioning system to treat 100% of the outdoor air. The proposed system was powered by solar energy and simulated using TRNSYS 16. The results, compared with conventional VAV (variable air volume) systems, showed a 51% saving in operating energy. Lee et al. [106] assessed the energy saving due to using LD in an evaporative cooling unit. The system consisted of LD/evaporative cooler, an electrical heater, and a cooling coil. TRNSYS and Engineering Equation Solver

(EES) were used to simulate the proposed system. An energy saving of 10–18% was estimated over a variable air volume system in summer in Seoul. Zhang et al. [107] studied an air conditioning system consisting of LD/evaporative cooling, in which LD removed the entire latent heat. The system was able to also handle a part of the sensible heat under specific climate zones. A theoretical model based on the NTU method for the heat exchangers was built to simulate the proposed system. The model showed a thermal COP (the ratio between system cooling capacity divided by the heat of regeneration) of 0.56.

In summary, LD-based air conditioning system is a promising alternative to vapor compression cycle, and tremendous work has been performed at the absorbent and system level to promote this technology. Although halide salt solutions have been extensively used due to their good performance, corrosion to many metal materials is a drawback. At the system level, packed beds have been used because they could provide good heat and mass transfer area. However, research and

development should focus on proposing new bed designs and innovative packing materials to enhance the heat and mass transfer performance, resulting in a significant improvement in the overall performance of the LD systems.

It is noticed that the desiccant-based air conditioning systems are thermally and/or electrically driven, making the comparison between different arrangements a challenge. Therefore, the primary COP, which is a unified factor, is formulated as shown in Eq. (1) and calculated for the reviewed works as listed in Table 2.

$$\text{Primary COP} = \frac{\text{System capacity}}{\dot{Q}_{th} + \frac{\dot{W}_{elec}}{cf}} \quad (1)$$

where \dot{Q}_{th} is the thermal energy, \dot{W}_{elec} is the electrical energy, and cf is the electrical-to-thermal conversion factor, which is 38% in this study [108].

3. Desiccant-based humidity pumps integrated into the building facade

The space requirement, fan energy usage, and regular maintenance of the ducting system are major drawbacks of conventional air conditioning systems [109–114]. Building-integrated heat pumps are considered stand-alone, oftentimes supplementary, space humidity

Table 2
The primary COP of desiccant-based SSLC systems.

System type	Desiccant material	Climate Conditions	Methodology	Primary COP	Ref.
Absorption	Silica gel	$T_e = 5\text{--}9^\circ\text{C}$, $T_c = 30^\circ\text{C}$	Modeling (MATLAB)	0.333–0.753	[29]
AB + DW	Silica gel in DW	Taxila, Pakistan	Modeling (TRNSYS)	0.458	[31]
DEC + DW	Silica gel	$T_a = 25\text{--}50^\circ\text{C}$,	Modeling (MATLAB)	0.104–0.215	[46]
DEC + DW		$RH_a = 4\text{--}98\%$.		0.162–0.478	
VCC + DW				0.136–0.601	
2 EC + DW	Silica gel	Moderate and humid, hot and	Modeling (TRNSYS)	0.63	[53]
M-cycle + DW				0.66	
2M-cycle + DW		semi-humid and hot and humid		0.728	
EC + SW + DW	NA	27°C and 49.6%	Exp. & modeling	0.591	[55]
EC + EW + DW	NA	Brisbane, Townsville, Darwin	Modeling (TRNSYS)	0.176–0.301	[56]
M-cycle + DW	Silica gel	UAE	Modeling	0.25–0.271	[62]
M-cycle + DW	Silica gel	Taxila, Pakistan	Experimental	0.65–1.17	[63]
M-cycle + DW	NA	Bandar Abbas, Iran	Modeling	0.389	[67]
DEC + DW	NA	Shanghai, China	Experimental	0.665	[69]
DEC + DW	NA	Shanghai, China	Modeling (TRNSYS)	0.453	[70]
2DEC + DW	Silica gel	Taxila, Pakistan	Experimental	0.283	[71]
DEC + IEC + DW				0.373	
2IEC + DW				0.694	
DEC + LD	CaCl ₂	$T_a = 34.6^\circ\text{C}$, $RH_a = 46\text{--}70\%$.	Experimental	0.411	[81]

AB: ABSorption cycle, DEC: Direct Evaporative Cooler, DW: Desiccant Wheel, EW: Enthalpy Wheel, IEC: Indirect Evaporative Cooler, LD: Liquid Desiccant, M-cycle: Maisotsenko Cycle, RH_a: Ambient relative humidity, SW: Sensible Wheel, T_a: Ambient temperature, T_c: Condenser temperature, T_e: Evaporator temperature, VCC: Vapor Compression Cycle.

management systems as they directly ab/adsorb indoor humidity using hygroscopic desiccant materials integrated into walls, ceilings, or windows. Humidity pumps, analogous to heat pumps, transfer humidity from a low to a high humid environment, thereby independently regulating the humidity level of living space. A humidity pump could robustly respond to the building's transient latent load without the need for large fans and ducts of an air conditioning system. Upon saturation of the desiccant material, humidity pumps employ various approaches, including a mechanical rotating mechanism or a liquid pump to regenerate the desiccant material. In the past decade, several architectural designs for humidity pump systems have been studied, as listed in Table 3 and discussed below.

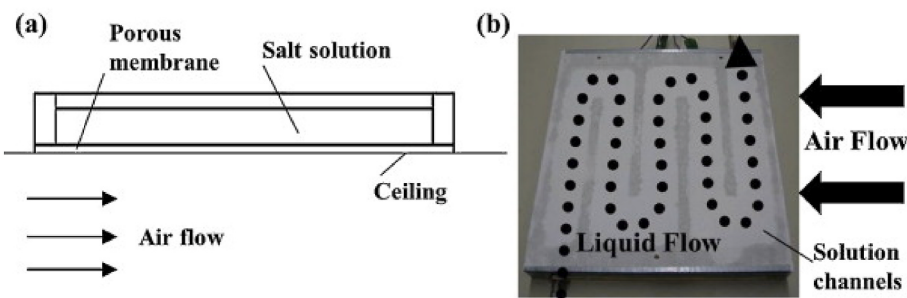
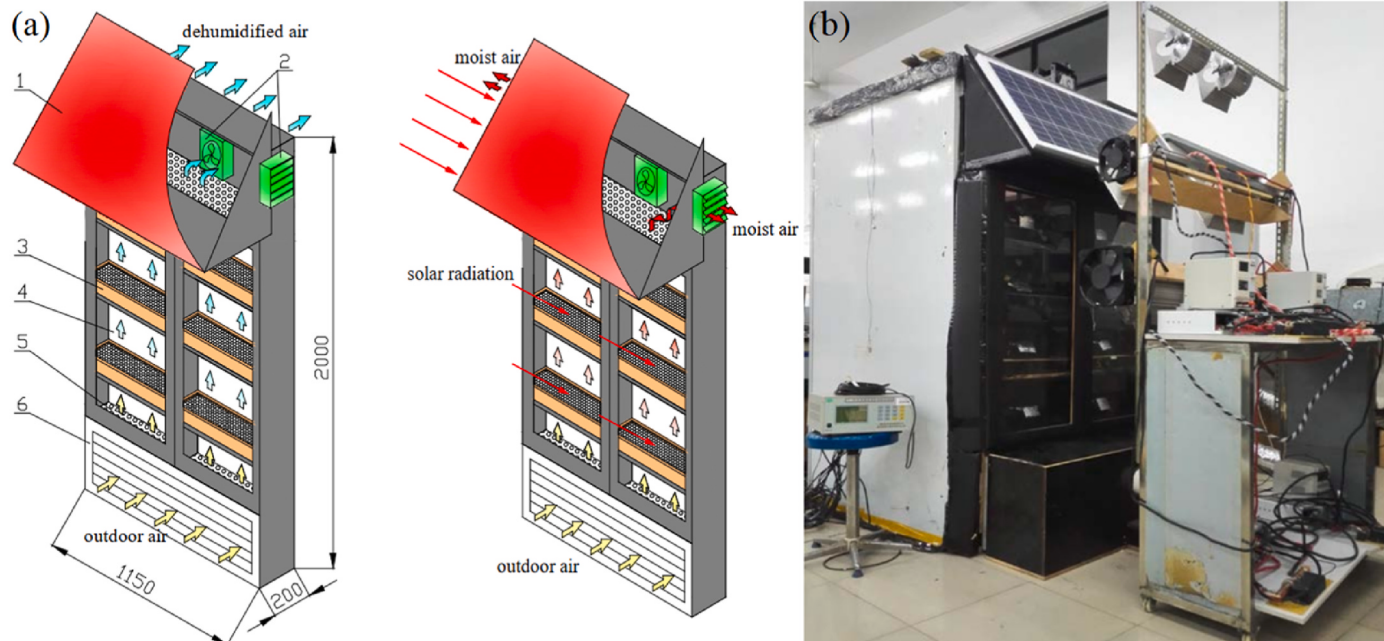
A building ceiling providing a large surface area is a promising candidate to be considered for liquid-desiccant-based humidity transfer panels. Inspired by radiating cooling panels (RCPs) [115–117], Fauchoux et al. [118] proposed a heat and moisture transfer panel (HAMP) to enable the humidification or dehumidification of a building environment. The HAMP, proposed to be integrated into the ceiling as shown in Fig. 11, employs LiCl flow channels constrained by a vapor venting membrane to manage the building humidity. A simulation study of a LiCl-based HAMP occupying 70% of a building ceiling area showed a 40% reduction in total energy usage compared to conventional AC systems in a hot and humid climate [119]. However, they did not consider the energy required for the regeneration process and the uniformity. Using solar energy to regenerate the liquid-desiccant LiCl solution, Keniar et al. [120] showed a 10% reduction in the relative humidity of office space using a direct membrane dehumidification system. Future studies need to focus on the performance and reliability of liquid-desiccant-based humidity transfer panels over a wider operating condition and with emerging non-corrosive ionic liquid solutions. Additionally, the long-term bonding reliability of vapor venting membranes over a large ceiling surface area needs to be examined.

Windows and external walls in buildings receive a large amount of solar energy that could be leveraged for the regeneration of desiccant materials employed in humidity pump systems. Yang et al. [121] proposed a solar-powered dehumidification window (SPDW) using silica gel embedded into a double-glazed window, as shown in Fig. 12. In the dehumidification mode, the humid outdoor air passing through the silica gel desiccant beads gets dehumidified and is then sent into the building indoor environment. In the regeneration mode, solar energy is employed to evaporate the adsorbed humidity molecules to the ambient. A lab-scale test prototype showed a maximum dehumidification efficiency of 58.6% with a maximum moisture removal rate of 7.1 g/kg. Zhang et al. [113] proposed a solar-driven humidity pump inspired by wood-like cellular networks. Using the low-priced and scalable electrospinning technique, a self-supporting and flexible MOF/LiCl desiccant layer was developed. As shown in Fig. 13, when the LiCl-rich MOF layer is shielded, the humidity from the indoor space is captured by the bottom side of the desiccant layer. Upon saturation, the top layer, coated with a photothermal solar absorbing material, is exposed to solar radiation for the desorption process. A proof-of-concept test setup showed that the indoor relative humidity could reduce from 70% to 55% under one sun illumination. Inspired by smart windows allowing a change in transparency properties of hydrogels in response to a temperature change [122–125], new hydrogels using humidity as a stimulus for a change in transparency are studied to enable both sensible and humidity load management. Nandakumar et al. [126] proposed a super hygroscopic hydrogel from a non-stoichiometric oxide of zinc blended with a glycol ether for a chromogenic coated smart window as shown in Fig. 14. The response of the hydrogel to a change in the humidity level enables a humidity pump action. When the indoor humidity level is high, the hydrogel absorbs humidity, thereby reducing the latent load. Simultaneously, the humidity absorption process results in the transition of the hydrogel material from a transparent to an opaque state. The low-transparent window then blocks a part of the incident infrared (IR) radiation which is beneficial to reduce the sensible load. During the

Table 3

A summary of desiccant-based humidity pumps integrated into building façade.

System type	Working principle	Desiccant material	Integration strategy	Working conditions	Effect on building energy metrics	Ref.
Humidity transfer panel	Liquid desiccant dehumidification	LiCl-Water	Panels in a building's ceiling	Covers 10% of the ceiling area, tested for four types of weather conditions	40% reduction in building total energy usage	[119]
Dehumidification window	Solar-driven solid desiccant dehumidification	Silica gel	Inside the wall thickness	Air relative humidity range: 74.2–86.1% and air mass flow rate range: 41.4–45.7 kg/h	Adding 10.7 °C to the air temperature	[121]
MOF-based humidity pump	Ad/desorption process	PAN/MIL @ LiCl	A window or wall-integrated module	Outdoor air RH: 46 and 80%, solar radiation flux: 1 kW/m ²	Regulating the indoor humidity level with one sun illumination to about 57% RH	[113]
Hydrogel smart window	Humidity-induced chromogenic	Non-stoichiometric oxide of zinc blended with a glycol ether	Rotating smart window	Outdoor air RH: 70%	Reducing the enclosed space RH to about 40%	[126]
Thermoelectric humidity pump	Heat pumping by the thermoelectric device	Silica gel	In the air handling unit	Outdoor air condition: RH: 67–98%, temperature: 21–34 °C	A 28.4 g/h humidity transfer rate without using a refrigerant or liquid	[127]
Thermoelectric humidity pump	Heat pumping by the thermoelectric device	MIL-100(Fe)	In the air handling unit	Outdoor air condition: RH: ~80%, temperature: ~23 °C	Moisture transfer rate: 34.9 g/h, dehumidification coefficient: 0.46, dehumidification efficiency: 1.14 gW/h	[128]

**Fig. 11.** (a) A side view, and (b) an actual image of the heat and moisture transfer panel (HAMP) [119].**Fig. 12.** (a) A schematic, and (b) an image of the solar-powered dehumidification window [121].

night, the window is rotated by 180° to reject the absorbed humidity molecules to the ambient by applying a small voltage. However, current systems show low moisture removal rates. Future studies should focus

on developing materials and systems with higher dehumidification rates per unit area to improve overall moisture removal capacity. Additionally, systems with fewer moving parts and simpler control mechanisms

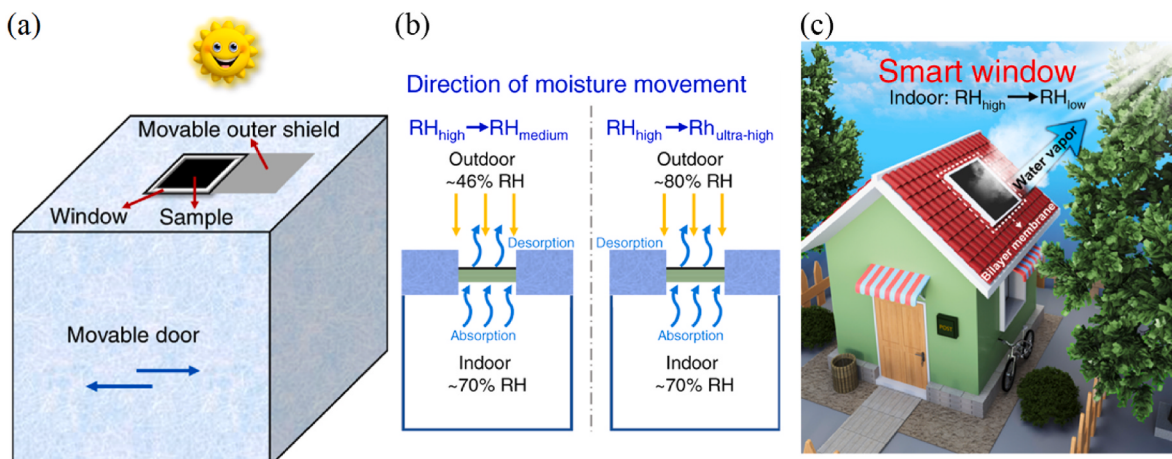


Fig. 13. (a) A schematic illustration of the moisture pump. The blue arrows represent the direction of door movement, (b) schematics displaying moisture movement through the moisture pump model to achieve indoor dehumidification, and (c) a smart window. (adapted from Ref. [113]).

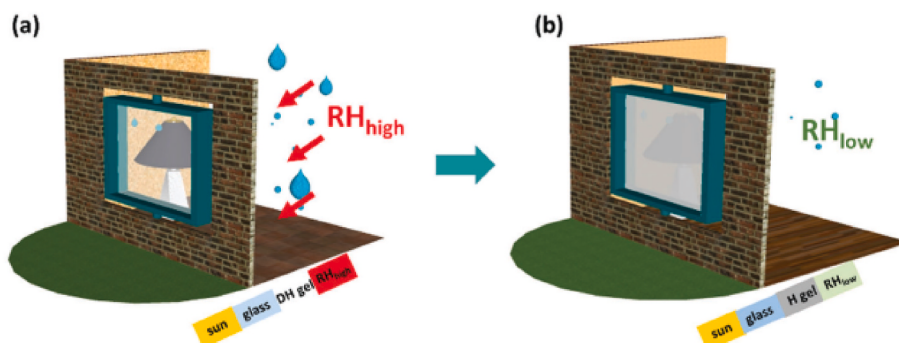


Fig. 14. A schematic of a window concept with a super hygroscopic hydrogel as a chromogenic material: (a) typical living space with high relative humidity, and (b) the hydrogel changes from a transparent to an opaque state upon humidity absorption [126].

are desired.

Solid-state thermoelectric humidity pumps with a coated solid desiccant material are also proposed to transfer humidity from a low to a high humid environment. The thermoelectric (TE) module transfers the adsorption heat released in the cold end to the hot end undergoing the regeneration process. Li et al. [127] proposed a solid-state humidity

pump, as shown in Fig. 15, to facilitate localized humidity control. The solid-state humidity pump consists of a TE module with two silica-gel-coated heat sinks and a mechanical rotation mechanism. Similar to other humidity pump approaches, the solid-state TE heat pump has a cyclic operation. In the first cycle, the desiccant-coated heat sink located in the cold end of the TE module is exposed to the indoor environment to capture the building humidity. The TE module transfers the heat of the adsorption process to the desiccant-coated heat sink in the hot end exposed to outdoor ambient to regenerate the humidity molecules adsorbed in the previous cycle. Upon completion of the adsorption and regeneration processes, the entire TE module is mechanically rotated to expose the saturated desiccant material to the outdoor ambient. Then, a change in the applied direct current voltage to the TE module results in the regeneration process in the hot outdoor end and the adsorption process in the cold indoor end of the TE module. To improve the heat and mass transfer performances of the thermoelectric humidity pump system, Hou et al. [128] proposed using a metal-organic framework (MOF) coated TE humidity pump. Their results showed that a MIL-100(Fe) desiccant system offers a moisture transfer rate of 34.9 g/h, which is approximately two times higher than that of silica-gel-based systems. The MOF TE-based humidity pump showed a dehumidification coefficient of performance of 0.46 and a dehumidification efficiency of 1.14 gW/h. The MOF-TE humidity pump successfully kept the relative humidity level of the indoor space at a comfortable level after about 15 min of operation without a significant increase in the temperature.

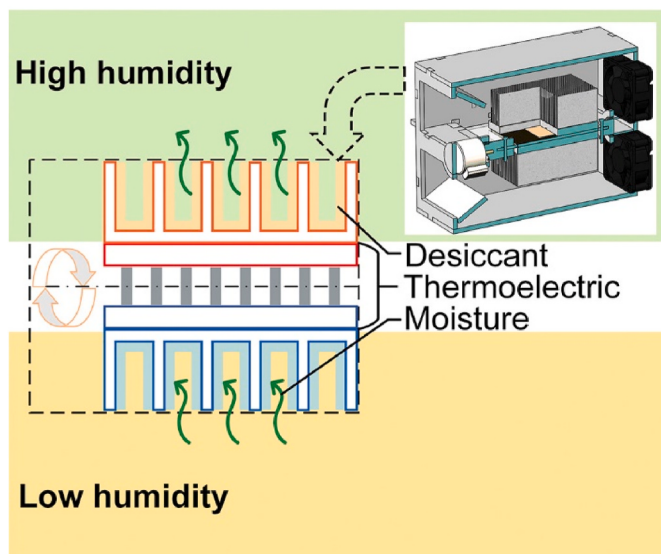


Fig. 15. A solid-state thermoelectric humidity pump [127].

4. Desiccant-based thermal energy storage systems

Thermal energy storage (TES) systems are paramount to shedding or shifting thermal loads in future sustainable buildings, thereby improving their overall energy efficiency. This is particularly important if the intermittent patterns of existing renewable energies and time-variant electricity pricing are considered. Sorption-based TES (STES) systems, in particular, are deemed promising due to their high energy storage densities at a low-to-medium temperature range suitable for building applications [129–138]. The high energy density of STES systems stems from their high enthalpy changes during reversible sorption reactions [139–148]. The other eminence of the STES systems is their long-term energy storage compatibility eliminating insulation strategies and thus enabling seasonal heat storage [149–153]. In a STES system, energy is stored during the endothermic desorption process (i.e., the charging state), where ad/absorbate is separated from ad/absorbent. Both hot and cold energies can be restored during the exothermic adsorption process (i.e., the discharging state), where the ad/absorbate is ad/absorbed by the ad/absorbent.

The STES systems can be generally classified into atmospheric (open) or sub-atmospheric (closed) systems [134,153,154]. In a sub-atmospheric closed configuration, only pure ad/absorbate molecules are present in the vapor phase. The closed-STES systems typically offer higher power density and temperature changes during heating and cooling modes compared to the open-STES configurations. This is because non-adsorbable gases such as nitrogen or oxygen molecules impeding the water vapor transport are absent, thereby resulting in higher water vapor mass transfer rates. Consequently, the closed-STES systems tend to be more compact [154]. The closed-STES systems, however, are expensive and require vacuum-proof components to maintain a pure ad/absorbate vapor phase state. On the other hand, non-ad/absorbable molecules present in the vapor phase deteriorate the ad/absorption mass transfer rate and power density of open-STES systems. To compare the potential of the different STES systems in buildings, prior research is presented in Table 4 and analyzed below in four groups sub-atmospheric solid-desiccant, atmospheric solid-desiccant, sub-atmospheric liquid-desiccant, and atmospheric liquid-desiccant TES systems.

4.1. Sub-atmospheric solid-desiccant TES systems

Removing the non-ad/absorbing molecules in the sub-atmospheric solid desiccant systems potentially leads to higher mass transfer rates, resulting in more compact systems. Finck et al. [155] developed a lab-scale thermochemical heat storage module for space heating applications. The sorption pair zeolite 5 A-water vapor was chosen for its hydrothermal/mechanical stability and corrosion minimization of heat exchanger surfaces. The system includes one adsorber/desorber unit and one evaporator/condenser unit. The ad/desorber module has a fixed bed design consisting of a finned heat exchanger in which the desiccant beads are adhered by a composite material to the substrate. The all-in-house fabricated system showed a space heating temperature span of 20–51 °C and a maximum energy density of 300 MJ/m³. Koll et al. [156] explored seasonal closed sorption thermal storage for hot water and space heating of a single-family house to address the mismatch between the abundant solar energy in summer and the heat demand in winter. Zeolite 13X and water vapor were chosen as the sorption working pair. The system was tested under a constant evaporator temperature of 20 °C and a storage temperature of 35 °C. Experimental results showed a heat storage density of 178 kWh/m³, which reduced the system size by three times compared to a sensible water storage system. Challenges associated with the non-condensable gases and the method to determine the state of the charge were two important take-aways. To increase the flexibility of STES systems, Li et al. [157] proposed a dual-mode thermochemical sorption energy storage system for seasonal solar thermal energy storage. Depending on the ambient winter

temperature, two discharging modes were designed to directly supply heat or create a temperature-lift heat supply. When the ambient temperature is relatively high, the heat released by both low and high-temperature units is directly used. When the ambient temperature is low, a heat transformer cycle is performed to achieve a high heat output temperature. To effectively use the solar thermal energy at below 100 °C, the working pair expanded graphite/SrCl₂–NH₃ was chosen. The reactors had a shell-and-tube configuration with ten finned tubes. The proposed system showed thermal energy densities of 706 kJ/kg and 305 kJ/kg at direct heating and temperature lift modes, respectively. To address the limited heat transfer in the material bed, Kant et al. [158] developed a mathematical model to study adsorption beds with cylindrical and rectangular fins. The heat and mass transfer equations were solved in the three-dimensional space using the finite element method. A parametric study was conducted to study the effect of geometrical parameters, including bed height, fin diameter/thickness, and fin spacing, on the energy discharge and peak power. The design-of-experiment study showed that the rectangular fin design offers better performance compared to the cylindrical fin design.

Fopah-Lele et al. [159] proposed a honeycomb heat exchanger design impregnated with desiccant material to avoid the agglomeration (gel-like formation) issue encountered in most heat storage systems based on thermochemical reactions. Thirteen dehydration-hydration cycles of SrBr₂·6H₂O were studied under low-temperature conditions (material temperatures <100 °C) for storage. The proposed system was successful in delivering an average air temperature of 22 °C for 4 h. The experimental data showed an energy density of 65 kWh/m³ and an efficiency of 77% with about 1 kg of desiccant material. Xu et al. [160] proposed a valve-less STES eliminating the large-diameter vacuum valve between the adsorber and the condenser/evaporator for vapor flow. The new design, shown in Fig. 16, decreases the cost, reduces the vapor flow resistance, and improves the system's reliability. Experimental results showed that the proposed STES with zeolite 13X/ENG-TSA and XM15/ENG-TSA sorbents achieve an energy efficiency of 0.38–0.49 under the charging temperature of 250 °C and the discharging temperature of 25–90 °C. Also, the energy storage density and maximum temperature lift of the STES are 120.3 kWh/m³ and 86.3 °C, respectively. The potential of using a highly porous metal-organic framework (MOF) in a STES system was investigated by Ehrenmann et al. [161]. Water uptakes of up to 1 g of water per gram of sorbent were reported for the 3D-[Cr₃F(H₂O)₂O (bdc)₃·~25H₂O] (MIL-101) material at temperatures of 40–140 °C under a water vapor pressure of 5.6 kPa. Also, the low regeneration temperature of 90 °C makes MIL-101 suitable for building thermal energy storage systems. The estimated sorption heat was determined to be 2.557 kJ/g. Their results showed the water uptake capacity degrades to 98.1% after 20 cycles and 96.8% after 40 cycles compared to the initial load. However, the utilization of MOF materials in fully functional and building-relevant-sized STES systems over a large number of cycles is yet to be realized.

The characterization and development of “salt-in-matrix” materials based on commercial mesoporous silica gels with embedded LiCl salt for seasonal TES systems were studied by Frazzica et al. [163]. The charging and discharging conditions were selected for two cold climatic zones of Central and Northern Europe. The detailed study on the textural properties of developed materials, including specific pore volume and pore size, helped define the optimal salt solution compositions to maximize the amount of impregnated salt. The storage density of the system was calculated based on the measured equilibrium isobars. The STES system with 30 wt% of LiCl offered a mass-based energy density of 1080 J/g_{ads}, which corresponds to a volumetric energy density range of 620–650 MJ/m³. Similar to MOF systems, the performance and reliability of salt-in-matrix systems need to be established at relevant sizes. Particularly, the leakage of the impregnated salt out of the host matrix pores is detrimental to salt-in-matrix STES systems. In summary, although sub-atmospheric solid-desiccant TES systems have a high potential for superior mass transfer rates resulting in more compact systems, the

Table 4

Desiccant-based thermal energy storage systems.

System type	System design	Desiccant material	System working parameters	Maximum heating/flow temperature	Energy density [unit]	Ref.
Sub-atmospheric solid desiccant-based TES	Packed bed in cylindrical SS vessel	zeolite 5 A-water	Regeneration temps: 80–120 °C and condenser temps: 20–30 °C	40 °C (for space heating) and 51 °C (for water heating)	300 MJ/m ³	[182]
	HX: U-formed copper pipes in star-shape assembly	Binder free zeolite 13XBF	Condenser temps: 15 and 20 °C and flowrate: 0.9 m ³ /h	31 °C	281 MJ/m ³	[183]
	Two temperature level discharging units	Expanded graphite/SrCl ₂ –NH ₃	Charging temperature: 94 °C discharging temperature: 15 °C (direct heating mode) and –15 °C (temperature lift mode)	35 °C (direct heating mode) 55 °C (temperature lift mode)	706 kJ/kg (direct heating mode) 305 kJ/kg (temperature lift mode)	[184]
	Finned adsorption bed	Silica gel	Condenser temperature: 30 °C Regeneration temperature: 30 °C Evaporator temperature: 10 °C	~80 °C	–	[185]
	Honeycomb heat exchanger	SrBr ₂ .6H ₂ O	Condenser temperature (charging): 16–20 °C HTF mass flow rate: 520 kg/h Charging temperature: 250 °C discharging temperature: 25–90 °C	43 °C	234 MJ/m ³	[186]
	Valve-less system design	Composites: zeolite 13X/ENG-TSA, XM15/ENG-TSA	Charging temperature: 250 °C discharging temperature: 25–90 °C	86.3 °C	432.9 MJ/m ³	[162]
	Feasibility study	MOF (MIL-101)	Charging temperature: 90 °C discharging temperature: 40 °C	–	1.6 GJ/m ³	[187]
Atmospheric solid desiccant-based TES	Thermodynamic evaluation	LiCl in silica gel porous matrix	Charging temperature: 85 °C discharging temperature: 35 °C evaporation temperature: 5 °C condenser temperature: 35 °C (for Central Europe) and 30 °C (for Northern Europe)	–	650 MJ/m ³	[188]
	Fixed bed	Composite: Activated alumina/LiCl	Air flow rate: 17–55 m ³ /h, air RH: 60–80% charging temperature: 110 °C	44.8 °C	687 MJ/m ³	[189]
	Honeycomb element	Composite: deposited LiCl on WSS	Air flow rate: 1–3 m ³ /h, regeneration temps: 60–120 °C	55 °C	180 MJ/m ³	[190]
	Rotating reactor Moving bed	Zeolite 4 A and MSX SrBr ₂ .H ₂ O/SrBr ₂ .6H ₂ O	Air flow rate: 140 m ³ /h Air flow rate: 80–140 m ³ /h, particle velocity: 0.5 and 1.5 cm/h	36 °C 41 °C	162 kJ/kg 4.57 kW/m ³	[191] [192]
	Fluidized bed	Silica gel	Air velocity: 2.3–4.7 m/s, particle dia.: 1.5–4.5 mm, air humidity: 4.5–10 g/kg	60 °C	–	[193]
	Multilayered sieve reactor	SrBr ₂ .6H ₂ O	Air velocity: 0.3–1 m/s, charging temperature: 85 °C, discharging temperature: 20 °C	~83 °C	Average: 800 W/m ³	[194]
	Buoyancy-driven quiescent single-tank Gravity-driven modules	CaCl ₂ NaOH	Charging temperature: 117–138 °C, ambient temperature: 20 °C Condenser temperature: 20 °C, evaporator temperature: 5 °C, and regeneration temperature: 120 °C	47 °C 70 °C	Theoretically 382 MJ/m ³ –	[52] [195]
Sub-atmospheric liquid desiccant-based TES	Combined one-shell design	LiBr	Condenser temperature: 10–20 °C, evaporator temperature: 5–10 °C, and regeneration temperature: 75–90 °C	42 °C	–	[179]
	Grooved vertical plate	KCOOH	Condenser temperature: 15 °C evaporator temperature: 15 °C absorber temperature: 20–30 °C regeneration temperature: 50–70 °C	Below 70 °C	–	[196]
	Multi-stage cycle	LiBr	Winter ambient temperature: 5 °C summer ambient temperature: 35 °C evaporator temperature: 2–16 °C regeneration temperature: 75–91 °C	50 °C	396.1 MJ/m ³ (double stage) 350.2 MJ/m ³ (triple stage)	[180]
	Compression-assisted	Ionic Liquid	Regeneration temperature: 70–100 °C evaporation temperature: 5 °C	–	576 MJ/m ³	[197]
	Internally cooled absorber	LiCl–H ₂ O	Air volumetric flow rate: 3000 m ³ /h inlet desiccant concentration: 39.7%	–	120 kWh/m ³ for cooling and 150 kWh/m ³ for dehumidification	[146]
	Multiple-stage system	LiBr–H ₂ O	Summer solar heat input temp.: 90 °C and ambient temp.: 35 °C	80 °C	Double stage: 396.1 MJ/m ³ and triple stage: 350.2 MJ/m ³	[180]
	Membrane-based modules	LiBr, LiCl, and CaCl ₂ aqueous solutions	Membrane area: 0.08 m ² , air flow rate: 0.75–1.125 m ³ /h	–	LiBr: 245 kJ/kg, LiCl: 350 kJ/kg, and CaCl ₂ : 306 kJ/kg	[189]

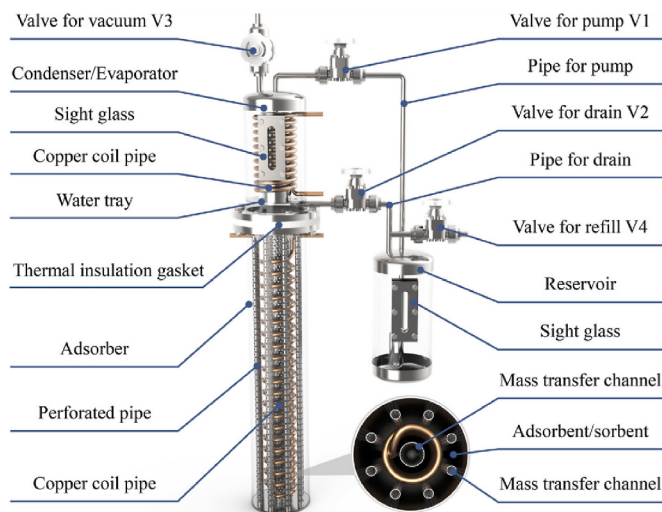


Fig. 16. A schematic of a valve-less sub-atmospheric solid desiccant system [162].

added complexity, high cost of vacuum-tight components, and relatively challenging and costly maintenance are among their drawbacks. These issues warrant additional studies. Of particular interest is to develop and examine building-relevant sized STES systems with new materials (such as MOFs) and approaches (such as salt-in-matrix systems) under an extended number of dehydration-hydration cycles.

4.2. Atmospheric solid-desiccant TES systems

In contrast to sub-atmospheric solid-desiccant TES systems, atmospheric solid-desiccant TES systems allow the AC air stream to flow directly through the desiccant media. In these systems, the thermal energy released during the adsorption process is directly transferred to the air stream. They also eliminate expensive vacuum-proof components. As such, they have gained popularity for residential building applications. The open atmospheric solid desiccant TES system has been studied since the 1970s [164,165]. To shed the electricity peak load in a residential building, Johannes et al. [166] designed and characterized a zeolite thermal energy storage open reactor. The Zeolite-13X beads with diameters ranging from 1.6 to 2.5 mm were chosen considering both the sorption capacity and economic aspects. Two packed bed reactors containing 80 kg of desiccant were connected to an air duct system. The system was able to supply thermal energy of 2.25 kW for 2 h. The effect of dehydration temperature, air flow rate, and air relative humidity was investigated on the heat storage performance. Zhang et al. [167] developed a 1 kW TES employing LiCl impregnated on the activated alumina composite sorbent for space heating. The system could use renewable energy, low-temperature waste heat, and off-peak electricity to charge the activated alumina/LiCl composite sorbent. In the charging mode, the heat associated with the output air can be reused for space heating. In the discharging mode, the adsorption heat is released to heat the room. The experimental data showed a maximum energy storage density of 191 kWh/m³ and a maximum system efficiency of 96.9%. To enhance the heat and mass transfer characteristics of fixed reactor STES systems, Liu et al. [168] proposed a composite honeycomb element based on the Wakanai Siliceous Shale (WSS) thermal energy storage and LiCl. The mesopores of the WSS were impregnated with 9.6 wt% LiCl. The proposed structure showed a low regeneration temperature (as low as 60 °C) and a high heat storage density of 180 MJ/m³ when it was regenerated at 80 °C. A novel multilayered sieve design based on a reversible solid-gas chemical reaction was investigated by Li et al. [169]. A 3D cubic reactor model was established to insert several metal sieve-plate beds packed with strontium bromide (SrBr₂) salt-hydrate

grains (grain size over 100-μm). Compared to the traditional bulk-packed reactors, the multilayered sieve design allows a better heat exchange and rapid evacuation of generated vapor during charging. The simulation results showed that an increase in top-to-bottom bed length and a decrease in bed-to-bed gap distance lead to higher performances. A thermal COP of 72.4% at charging and 71.5% at discharge was calculated. The non-uniform flow distribution was detected as the main issue of the proposed system.

To tackle the low heat and mass transfer performance of fixed bed systems, alternative reactor designs have been proposed. Moving material beds, for instance, were proposed to address the lack of volumetric involvement of solid desiccant media in fixed reactor beds. Zettl et al. [170] studied a rotating reactor system as an open sorption thermal storage process for space and water heating. The rotating reactor bed includes a rotating cylindrical drum made of zeolite 4 A and zeolite MSX with air blown through the rotating bed. The test results showed a thermal storage capacity of 162 kJ/kg, which is about 90% of the theoretical potential. Farcot et al. [171] examined a moving-bed thermochemical reactor with SrBr₂/H₂O pair for solar heat storage in buildings. As shown in Fig. 17, falling solid desiccants and humid air interact in a cross-flow configuration. Reactor bed temperatures as high as 41 °C and specific heating powers ranging from 1.7 to 4.57 kW/m³ were obtained. This study highlighted the impact of air humidity at the reactor inlet on the reactor performance. A fluidized bed configuration is another proven method to enhance heat and mass transfer rates of sorption bed systems.

Rogala et al. [172] studied the performance of silica gel-water adsorption and desorption of air-fluidized systems. Experiments were conducted to evaluate the effect of working parameters, including air temperature, humidity, superficial velocity, and silica gel particle diameters, on the adsorption and desorption performance. It was found that the kinetics of the adsorption process is enhanced by an increase in the air superficial velocity, a decrease in the particle diameter, and an increase in the air humidity. The mass transfer mechanisms limiting the air-fluidized silica gel-water adsorption and desorption processes are identified as air-to-air film mass convection and intra-particle mass diffusion, respectively. In summary, the open atmospheric solid-desiccant TES systems are attractive for residential building applications as they eliminate the need for expensive vacuum-proof components and environmentally harmful refrigerants. Future research and development endeavors should focus on the major drawbacks of the atmospheric solid-desiccant TES systems, including bulkiness, high air circulation power consumption, scalability, and dependency, on outdoor air conditions.

4.3. Sub-atmospheric liquid-desiccant TES systems

Liquid-desiccant-based TES systems are attractive as they enable thermal energy recovery between absorption and desorption processes leading to higher thermal COPs, and offer higher absorption and air dehumidification rates per unit of desiccant weight compared with the solid-desiccant-based TES systems. Particularly, under a sub-atmospheric environment, liquid-desiccant TES systems allow substantially high absorption rates resulting in highly compact liquid-desiccant TES systems. However, existing liquid-desiccant TES systems suffer from sorbent flow maldistribution, thick sorbent films, and corrosion issues.

In an attempt to evaluate the long-term storage feasibility of solar heat in closed liquid-desiccant TES systems, Weber and Dorer [173] analyzed the performance of a prototype TES system using sodium hydroxide (NaOH)-water as the working pair. The system employs dish-shaped heat exchangers with gravity-driven desiccant flow for absorption and desorption processes. It was found that a minimum required temperature of 120 °C for solar heat input is required. The volume-based heat storage density of the system is three times that of conventional water storage at a domestic hot water supply at 65–70 °C. Quinnell and Davidson [174] proposed a single-vessel desiccant tank

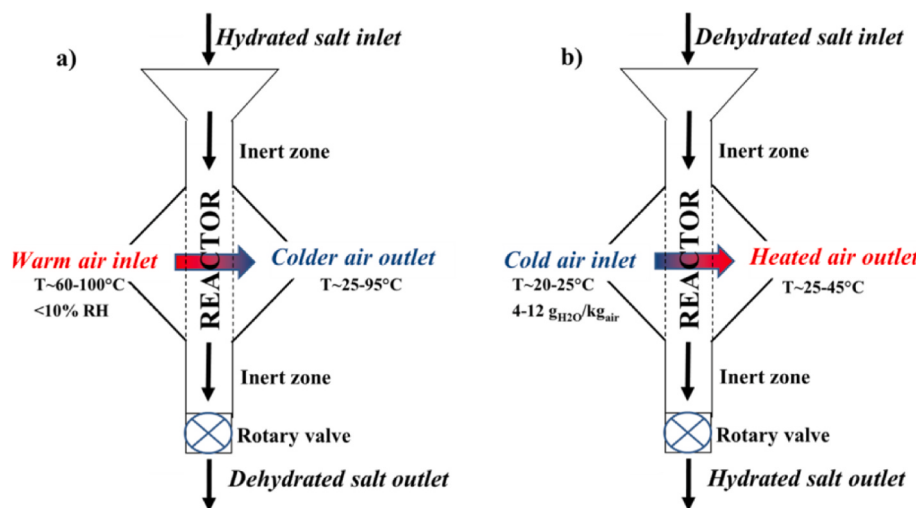


Fig. 17. A schematic of a moving-bed thermochemical reactor (a) charging mode and (b) discharging mode [171].

storing the sensible energy for short timescales and the binding energy of the absorption process for seasonal timescales. The long-term energy storage was enabled by the natural density difference between the charged (i.e., concentrated sorbent) and discharged calcium chloride solutions to avoid mixing. An immersed vertical tube heat exchanger and stratification manifold added energy and fluid, respectively. The results showed that, for Sherwood numbers between 35 and 62, the absorption time constants are between 160 and 286 days, which are longer than typical seasonal storage timescales for a cold climate.

Zhang et al. [175] studied the dynamic performance of a closed liquid-desiccant TES system during charging and discharging modes. The 10-kWh system employed the LiBr–H₂O pair as the working fluid and under sub-atmospheric pressures. It was found that higher charging and lower discharging temperatures result in higher heat storage capacities. The LiBr–H₂O TES system showed energy storage densities of 42, 88, and 110 kWh/m³ energy densities for cooling, hot water heating, and space heating, respectively. The effect of added expanded graphite (EG) in a LiCl TES system was examined by Zhao et al. [176] for space and water heating applications in family houses. The added EG improves the heat and mass transfer characteristics of the composite sorbent solution. Under a charging temperature of 85 °C, discharging temperature of 40 °C, condensing temperature of 18 °C, and evaporation temperature of 30 °C, a heat storage capacity of 10.25 kWh was obtained. The sorption heat accounted for 60% of the total heat storage capacity. This resulted in a heat storage density of 65.29 kWh/m³, which is two times higher than that of a sensible water heat storage system.

To leverage the energy associated with the sorbent crystallization process and increase the energy storage density, N'Tsoukpoe et al. [177] developed a TES prototype based on the LiBr-water pair as the working fluid. Fig. 18 shows an image of the prototype with one reactor and two separate storage tanks for solution and water. To reduce the vapor pressure drop, the falling film absorber-desorber and evaporator-condenser modules were combined into the same shell. Both static and dynamic operating conditions of the system were investigated. The solution flow rate was identified as the most influential parameter affecting the desorber heat transfer rate. Under a desorber charging temperature of 25–95 °C and condenser temperature of 10–30 °C, a maximum charged heat storage capacity of 13 kWh was achieved. In a follow-up study, Pierres et al. [178] examined the performance of the TES system employing KCOOH–H₂O couple as the working fluid. The KCOOH sorbent is more cost-effective and shows lower corrosion rates than the LiBr sorbent for heat storage applications. However, the performance of the KCOOH–H₂O pair is slightly lower than that of the LiBr–H₂O couple. The KCOOH–H₂O pair showed discharging

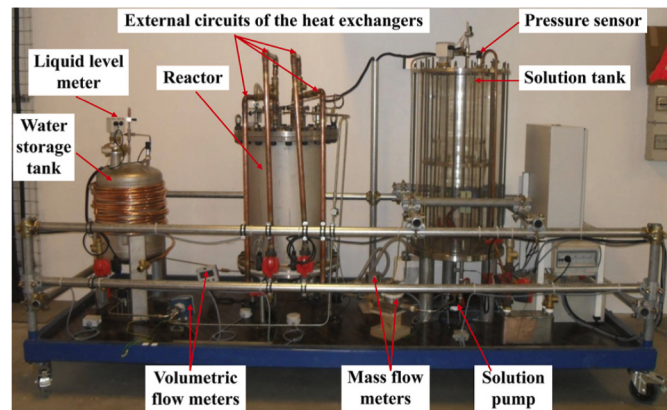


Fig. 18. An image of a vacuum-tight liquid-desiccant heat storage system [179].

temperatures lower than 30 °C, which might be only suitable for space heating and not for domestic hot water application.

A multi-stage sorption cycle is one of the established approaches to improving the energy efficiency of sorption systems. Compared to single-stage sorption systems, multi-stage counterparts allow a larger concentration span, resulting in higher energy storage densities. Xu and Wang [180] analyzed the performance of double and triple-stage liquid-desiccant TES systems employing LiBr-water pair as the working fluid. The modeling results showed the double-stage system outperforms the triple-stage system under the same charging temperature. Under typical summer solar thermal charging and winter heat demand temperature of 50 °C, the energy storage densities of the double and triple-stage sorption cycles are 7.32 (i.e., 254.0 kJ/kg) and 6.78 times (i.e., 235.5 kJ/kg) higher than that of the single-stage sorption cycle, respectively.

To reduce corrosion and crystallization issues associated with conventional liquid-desiccant solutions, Wu [181] proposed a hybrid compression-assisted liquid-desiccant TES system using Ionic Liquids (IL) as the desiccant media. The performance of the system was investigated using four ILs ([DMIM][DMP], [EMIM][Ac], [EMIM][DEP], and [EMIM][EtSO₄]) and a reference LiBr aqueous solution. The system was equipped with a compressor between the evaporator/condenser and absorber/desorber modules to increase the absorption pressure and decrease the regeneration pressure. The [EMIM][Ac]-water and [EMIM][EtSO₄]-water pairs showed the highest energy storage density at

regeneration temperatures above and below 86 °C, respectively. In summary, the sub-atmospheric liquid-desiccant TES systems offer high absorption and desorption rates, leading to high energy storage densities and compact TES systems.

4.4. Atmospheric liquid-desiccant TES systems

Atmospheric liquid-desiccant TES systems are a simpler alternative to sub-atmospheric liquid-desiccant TES systems as they eliminate costly vacuum-proof components. The ability of the AC air stream to directly interact with the liquid desiccant media could be considered an advantage as it removes the need for a secondary heat exchanger module. Here, the liquid-desiccant solution can be first concentrated through the desorption process enabled by available thermal energy sources, including solar energy and waste heat. The concentrated liquid-desiccant solution can then interact with a humid air stream to resume the stored chemical energy in the form of thermal energy through the absorption process.

Kabeel et al. [152] studied an open solar-driven liquid-desiccant system. The liquid-desiccant system allows storing of chemical energy in the liquid desiccant or thermal energy in the heating water. A transient model was employed to predict the system performance under thermal energy storage, thermochemical energy storage, and combined thermal and thermochemical energy storage modes. The results showed that the combined energy storage method is the most energy-efficient method with the lowest electric energy consumption. Wang et al. [151] proposed a solar-driven membrane-based liquid-desiccant TES system. Solar energy was employed to regenerate the liquid desiccant solution and store energy as the concentration gradient. The hollow fiber membrane module, shown in Fig. 19, offers a high specific surface area increasing the energy density of the system. The experimental results showed energy storage densities of 245, 350, and 306 kJ/kg when LiBr, LiCl, and CaCl₂ solutions were concentrated from 50% to 55%, from 35% to 40%, and from 40% to 45%, respectively. However, there are very limited studies focusing on atmospheric liquid-desiccant TES systems. Therefore, additional research and development efforts are

warranted to study the physics and performance of atmospheric liquid-desiccant TES systems under various atmospheric conditions and sorption cycle operating conditions.

5. Desiccant-based appliances for future buildings

There is a growing interest in leveraging desiccant materials to improve the energy efficiency and overall functionality of building appliances [198–201]. Desiccants are particularly advantageous for appliances with high-humidity contents. The high enthalpy of ab/adsorption and regeneration processes can be seen as a potential source of energy to increase the overall energy efficiency of several building appliances. Two major energy-hungry building appliances known for their high humidity generation rates are clothes dryers (CD) and dishwashers.

Standard clothes dryers consume a significant amount of energy to heat the ambient air entering the drum. The hot and dry air drives the fabric drying process resulting in warm and humid air at the drum outlet. In conventional vented clothes dryers, the high enthalpy of the warm and humid leaving the drum is wasted to ambient. More advanced clothes dryers use a vapor compression heat pump (VCHP) to recuperate a part of the energy associated with the vented air and thus increasing the energy efficiency. In a VCHP-CD, the evaporator module of the heat pump cycle reduces the air temperature to its dew point to enable dehumidification of the warm and humid air leaving the drum. The cold and dry air is then passed through the condenser coil of the heat pump cycle to be heated before being sent back to the drum, as shown in Fig. 20a. Cranston et al. [202] examined the use of a desiccant material in combination with the vapor compression heat pump cycle in a clothes dryer. The proposed hybrid system integrates a sorption bed between the evaporator and condenser modules of the heat pump clothes dryer, as shown in Fig. 20b. In this configuration, the cold dry air is further dried by the sorption bed before entering the condenser to be heated. The sorption bed employing a composite desiccant material of the [emim][CH₃SO₃] ionic liquid confined in Syloid AL 1FP silica pores showed a 19-min reduction in drying time and a 6% reduction in drying

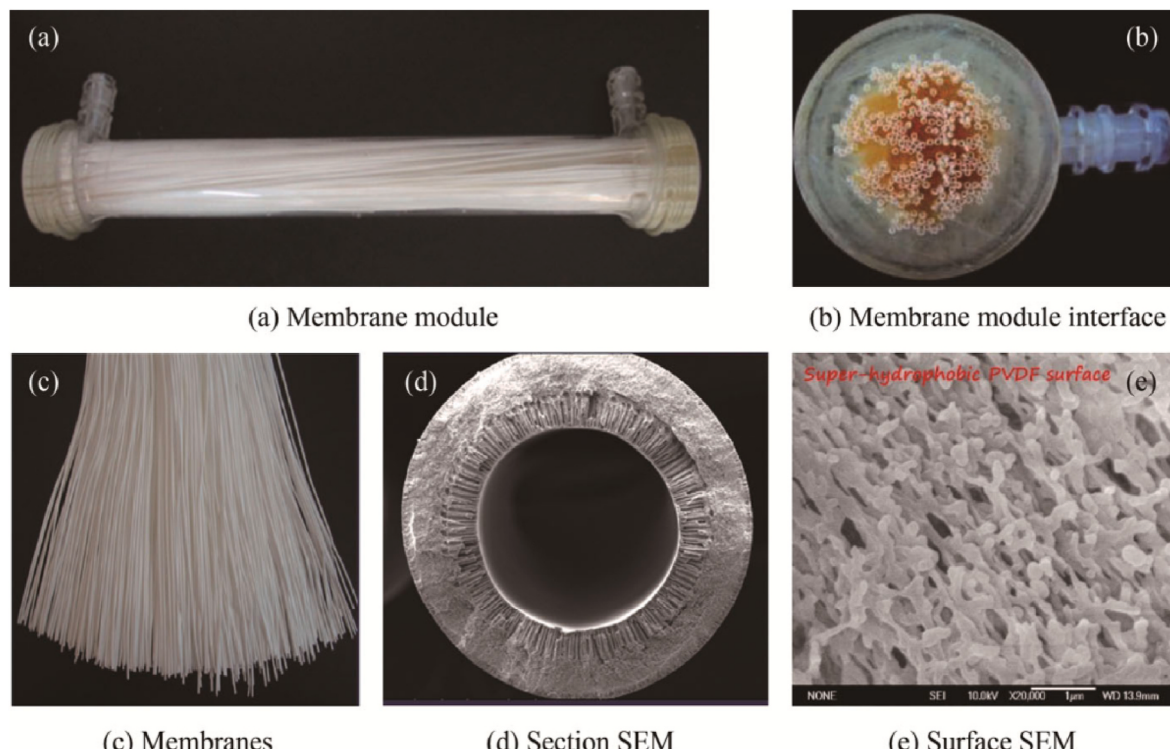


Fig. 19. Images of the membrane-based liquid-desiccant TES module [151].

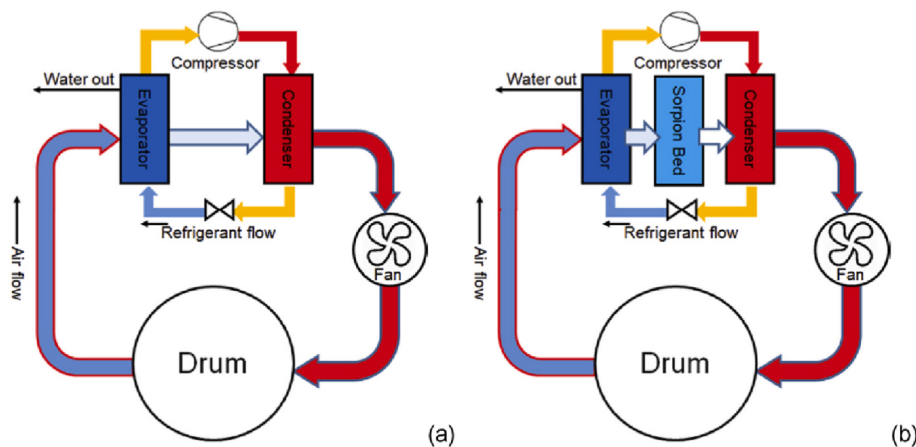


Fig. 20. Schematics of (a) a VCHP and (b) a sorption-assisted VCHP clothes dryer [202].

energy usage. Alternatively, desiccant-based thermal energy storage is considered to enhance the energy efficiency of clothes dryer systems. El Fil and Garimella [203] utilized an adsorbent bed in the exhaust stream of a clothes dryer to store the thermal energy in the form of thermochemical potential and reuse it in subsequent drying cycles. They showed an almost 6-min reduction in drying time and an 18.2% reduction in the dryer energy consumption when the effects of exhaust gas recirculation and a 5-kg silica gel bed were combined. Future investigations could focus on novel desiccant bed architectures to further improve the adsorption rate and reduce the air-side pressure drop penalty. Additional studies are also required to consider the regeneration energy required for the sorption bed for consecutive drying cycles.

To overcome the drawbacks of existing standard and VCHP clothes drying systems, a novel liquid-desiccant heat pump dryer concept was recently proposed by Ahmadi et al. [199]. A schematic of the liquid-desiccant heat pump dryer is shown in Fig. 21. Unlike the VCHP clothes dryers, where the dehumidification process occurs at a low dew-point temperature, the proposed liquid-desiccant heat pump dryer drives the dehumidification process at an elevated temperature. Here, the warm and humid air leaving the drum is sent to a liquid-desiccant dehumidifier module to be dehumidified at high temperatures. In other words, the proposed liquid-desiccant clothes dryer does not deteriorate the sensible heat of the warm and humid air for the dehumidification process. On the contrary, the heat released during the absorption process further increases the sensible heat of the dehumidified

air and thus making it more suitable for the drying process. Furthermore, the heat of the condensation process is also transferred to the air flow stream to further increase its temperature to a hot dry air state before flowing back to the drum. Consequently, the proposed sorption-based dehydration system effectively utilizes the latent heat associated with the moisture twice: once during the dehumidification and again during the subsequent condensation process. The double utilization of the latent heat associated with the humidity in the sorption-based heat pump dryer results in a 112% improvement in the drying energy efficiency compared with existing vented clothes dryers. The proposed sorption-based clothes dryer also eliminates the need for environmentally harmful refrigerants and expensive vacuum-based components present in VCHP clothes dryers. Future research could focus on the performance evaluation of the proposed system with non-corrosive, non-crystallizing ionic liquid solutions. Additional investigations are also required to better understand the performance of the liquid-desiccant heat pump dryer under non-standard fabric loading conditions.

Hauer et al. [204] proposed an open adsorption system to reduce the energy consumption of a dishwasher. In conventional dishwashers, an electric water heater increases the water temperature for the washing process. The heat capacity of the dishes drives the dish drying process at a temperature above 60 °C. In the adsorption-based dishwasher, the humidity of the hot and humid air leaving the 13X zeolite sorption bed during the regeneration period condenses on the cold water and the dishes. The latent heat of the condensation process heats up the water and the dishes for the washing process. During the dish-drying process, the humid air from the dishwasher is sent to the regenerated zeolite-packed bed to become hot and dry. The hot and dry air drives the dish-drying process. The performance evaluation of the proposed adsorption-based dishwasher showed about a 24% reduction in energy consumption compared with conventional dishwashers. However, the very high hydrophilic nature of 13X zeolite results in high regeneration energies (>4000 kJ/kg) and high regeneration temperatures above 250 °C, which may induce significant thermal stresses to components of dishwater [205]. Santori et al. [205] explored the energy efficiency of dishwater with various desiccant materials, including microporous silica gel and SAPO-34 zeolite, exhibiting lower regeneration temperatures, lower desorption enthalpies, and sufficiently high adsorption capacities compared with the 13X zeolite. They reported electrical energy consumption of 0.636 kWh with the silica gel desiccant material in an optimized dishwasher configuration, a 41% reduction in energy consumption compared with a standard dishwasher. Hauer and Fischer [206] proposed the dishwasher shown in Fig. 22 based on an open adsorption cycle, aiming to reduce energy consumption. Zeolite 13X was used as an adsorbent. Air was heated during the regeneration process and used to dry the dishes. This approach led to a 25% reduction in

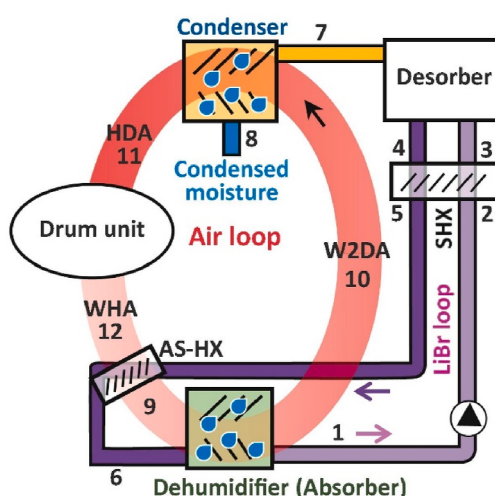


Fig. 21. A schematic of a liquid-desiccant-based heat pump clothes dryer [199].

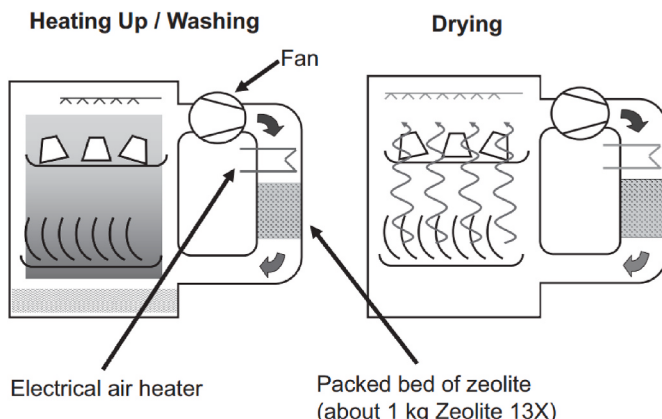


Fig. 22. A schematic of an adsorption-integrated dishwasher [206].

energy consumption compared to conventional dishwashers. Future studies should focus on overall system optimization as well as performance evaluation of the adsorption-based dishwashers with advanced desiccant materials inducing metal-organic frameworks.

6. Opportunities, challenges, and future prospectives

Desiccant-based technologies have shown to be promising candidates for improving the energy efficiency and functionality of future buildings. In particular, desiccants offer an independent moisture management method that separates sensible and latent cooling (SSLC) loads. Employing sorption technologies to remove the sensible loads is still at a low technological readiness level due to the low thermal diffusivity of adsorbents. Coupling desiccant-based dehumidification with VCC systems offers a promising integration synergy as the desiccant system can handle the latent load, and the VCC system is responsible for the sensible load. Harvesting the heat of condensation to regenerate the desiccant materials is found to be an energy-efficient approach to improving the overall system performance. Also, desiccant-based humidity pumps are envisioned as complementary space humidity management systems as they passively/actively ab/adsorb indoor humidity using hygroscopic desiccant materials integrated into walls, ceilings, or windows. A humidity pump could robustly respond to the building's transient latent load without the need for large fans and ducts of an air conditioning system. Additionally, sorption-based thermal energy storage systems could play a significant role in shedding or shifting thermal loads in future buildings as they offer high energy densities during reversible sorption reactions and long-term energy storage compatibility. Furthermore, desiccants are deemed promising materials improving the energy efficiency and overall functionality of modern appliances in future buildings.

Desiccant materials obviously have the potential to be an integral part of future buildings, either actively or passively, if the remaining scientific and economic aspects of desiccant-based technologies are addressed. Future research and development activities on liquid-desiccant-based air conditioning, TES, humidity pump, and appliance technologies should focus on improving liquid-desiccant flow distributions for augmented absorption and desorption processes, developing durable coating strategies for reduced corrosion and crystallization issues, improving thermo-hydraulic properties of emerging ILs, and reducing the overall costs and complexities of sub-atmospheric liquid-desiccant systems. Liquid desiccant mal-distribution could significantly reduce the absorption and desorption rates but could be addressed by textured absorber/desorber surfaces [11] or membrane-based absorber/desorber modules [9]. However, the long-term bonding reliability of vapor venting membranes over a large surface area needs to be improved. Future research and development activities on solid-desiccant-based air conditioning, TES, humidity pump, and

appliance technologies should improve the low thermal conductivity of solid desiccants for rapid cooling during the adsorption or heating during the regeneration process, enhance thermal and chemical stabilities of solid desiccants, and augment adsorption and regeneration rates to further reduce the size of solid-desiccant-based systems. Air mal-distribution could negatively affect the adsorption and regeneration rates but could be potentially addressed through 3D-printed solid-desiccant topologies [10]. Additional research and development are also required to enable directional passive humidity management in future buildings. New materials (such as MOFs) and approaches (such as salt-in-matrix systems) have shown some promising results in lab scales under narrow operating ranges or a limited number of dehydration-hydration cycling and warrant further development under wider operating ranges and an extended number of cycles.

7. Conclusions

The present review paper focused on the potential of desiccant-based technologies to achieve indoor air quality, thermal comfort, and energy saving in future buildings. Four major areas of desiccant-based air conditioning systems, thermal energy storage systems, humidity pumping, and appliances were considered. A particular focus of current research is on hygroscopic desiccant materials separating the latent and sensible cooling loads in modern air conditioning units to enhance the overall system performance. Ad/absorption and desorption cycles handle the latent cooling while the evaporator module of the VCC unit is responsible for the sensible cooling load.

A great deal of recent research has focused on the development of humidity pumps, in which desiccant materials are integrated into the building facade to control indoor humidity without the need for large fans and ducts of an air conditioning system. Several architectural designs for humidity pump systems were studied and discussed. MOFs were found to be a good candidate for humidity pumping due to their high adsorption capacity and their capability of controlling indoor humidity in a short period. Desiccant materials have also been shown to be promising candidates for TES applications shedding or shifting thermal loads in future buildings, thereby improving their overall energy efficiency. Open atmospheric solid-desiccant TES systems are more attractive as they avoid the need for expensive vacuum-proof components and environmentally harmful refrigerants. Additionally, several recent studies showed that desiccant materials enhance energy efficiency and overall functionality of building appliances, particularly for appliances with high-humidity contents such as clothes dryers and dishwashers. Furthermore, the present review paper highlights several shortcomings of desiccant-based technologies that need to be overcome in future studies for commercial viability and widespread acceptance of desiccant-based systems.

Declaration of competing interest

The authors declare that they have no known competing financial interests or personal relationships that could have appeared to influence the work reported in this paper.

Data availability

Data will be made available on request.

Acknowledgments

This study was partially sponsored by the US Department of Energy's Office of Energy Efficiency and Renewable Energy (EERE) under the Building Technology Office Award Number DE-EE0008685. M.A. and S. B. would like to acknowledge Mr. Antonio Bouza and Mr. Mohammed Khan, Technology Managers, and Mr. Michael Geocaris and Mr. Andrew Kobusch, Project Engineers, HVAC, Water Heating, and Appliance

subprogram, Building Technologies Office, US Department of Energy.

References

- [1] Tian S, Su X, Geng Y. Review on heat pump coupled desiccant wheel dehumidification and air conditioning systems in buildings. *J Build Eng* 2022;54:104655. <https://doi.org/10.1016/J.JBODE.2022.104655>.
- [2] Frequently Asked Questions (FAQs) - U.S. Energy Information Administration (EIA) n.d. <https://www.eia.gov/tools/faqs/faq.php?id=86&t=1> (accessed July 31, 2022).
- [3] Buildings – Topics - IEA n.d.. <https://www.iea.org/topics/buildings>. [Accessed 31 July 2022].
- [4] United Nations. The Sustainable Development Goals Report 2022, Department of Economic and Social Affairs (DESA) e-ISSN. 2022. p. 251–3958.
- [5] Aziz MA, Gad IAM, Mohammed ESFA, Mohammed RH. Experimental and numerical study of influence of air ceiling diffusers on room air flow characteristics. *Energy Build* 2012;55:738–46. <https://doi.org/10.1016/j.enbuild.2012.09.027>.
- [6] Basic Facts about Mold and Dampness | CDC n.d. <https://www.cdc.gov/mold/faqs.htm> (accessed July 31, 2022).
- [7] Habib MF, Ali M, Sheikh NA, Badar AW, Mehmood S. Building thermal load management through integration of solar assisted absorption and desiccant air conditioning systems: a model-based simulation-optimization approach. *J Build Eng* 2020;30:101279. <https://doi.org/10.1016/J.JBODE.2020.101279>.
- [8] Singh G, Das R. Energy saving potential of an air-conditioning system with desiccant and solar assisted ventilation. *Lecture Notes in Mechanical Engineering*, Springer 2020:1351–9. https://doi.org/10.1007/978-981-15-0124-1_119.
- [9] Ahmadi B, Ahmadi M, Nawaz K, Momen AM, Bigham S. Performance analysis and limiting parameters of cross-flow membrane-based liquid-desiccant air dehumidifiers. *Int J Refrig* 2021. <https://doi.org/10.1016/j.ijrefrig.2021.09.010>.
- [10] Puttur U, Ahmadi M, Ahmadi B, Bigham S. A novel lung-inspired 3D-printed desiccant-coated heat exchanger for high-performance humidity management in buildings. *Energy Convers Manag* 2022;252:115074. <https://doi.org/10.1016/j.enconman.2021.115074>.
- [11] Ahmadi M, Ahmadi B, Bigham S. Wickability-optimized textured liquid-desiccant air dehumidifiers for independent moisture management in energy-efficient buildings. *Energy Convers Manag* 2022;260:115637. <https://doi.org/10.1016/j.enconman.2022.115637>.
- [12] Mohammed RH, Mesalhy O, Elsayed ML, Huo R, Su M, Chow LC. Performance of desiccant heat exchangers with aluminum foam coated or packed with silica gel. *Appl Therm Eng* 2020;166. <https://doi.org/10.1016/j.aplthermaleng.2019.114626>.
- [13] Sahlot M, Riffat SB. Desiccant cooling systems: a review. *Int J Low Carbon Technol* 2016;ctv032. <https://doi.org/10.1093/ijlct/ctv032>.
- [14] Scopus - Analyze search results n.d. <https://www.scopus.com/term/analyzer.uri?sid=ddcf71ba90143e0b6d397f31e033bc3&origin=resultslist&src=s&s=%28TITLE-ABS-KEY%28desiccant%29+AND+TITLE-ABS-KEY%28buildings+OR+space+or+room+or+zone%29%29+sort=plf-f&sdt=b&sot=b&sl=80&count=1326&analyzeResults=Analyze+results&txGid=d72aa7cce546fb61526284f86f03abbb> (accessed July 31, 2022).
- [15] Mohammed RH, Rezk A, Askalany A, Ali ES, Zohir AE, Sultan M, et al. Metal-organic frameworks in cooling and water desalination: synthesis and application. *Renew Sustain Energy Rev* 2021;149:111362. <https://doi.org/10.1016/j.rser.2021.111362>.
- [16] Mohammed RH, Rashad E, Huo R, Su M, Chow LC. Pore-size engineered nanoporous silica for efficient adsorption cooling and desalination cycle. *NPJ Clean Water* 2021;4. <https://doi.org/10.1038/s41545-021-00129-y>.
- [17] Abd-Elyahdy MM, Salem MS, Hamed AM, El-Sharkawy II. Solid desiccant-based dehumidification systems: a critical review on configurations, techniques, and current trends. *Int J Refrig* 2022;133:337–52. <https://doi.org/10.1016/j.ijrefrig.2021.09.028>.
- [18] Venegas T, Qu M, Nawaz K, Wang L. Critical review and future prospects for desiccant coated heat exchangers: materials, design, and manufacturing. *Renew Sustain Energy Rev* 2021;151:111531. <https://doi.org/10.1016/j.rser.2021.111531>.
- [19] Bai HY, Liu P, Justo Alonso M, Mathisen HM. A review of heat recovery technologies and their frost control for residential building ventilation in cold climate regions. *Renew Sustain Energy Rev* 2022;162:112417. <https://doi.org/10.1016/j.rser.2022.112417>.
- [20] Ahmadi M, Gluesenkamp KR, Bigham S. Energy-efficient sorption-based gas clothes dryer systems. *Energy Convers Manag* 2021;230:113763. <https://doi.org/10.1016/j.enconman.2020.113763>.
- [21] Guan B, Zhang T, Liu J, Liu X, Yin Y. Review of internally cooled liquid desiccant air dehumidification: materials, components, systems, and performances. *Build Environ* 2022;211:108747. <https://doi.org/10.1016/J.BUILDENV.2021.108747>.
- [22] Salikandi M, Ranjbar B, Shirkan E, Shanmuga Priya S, Thirunavukkarasu I, Sudhakar K. Recent trends in liquid desiccant materials and cooling systems: application, performance and regeneration characteristics. *J Build Eng* 2021;33:101579. <https://doi.org/10.1016/J.JBODE.2020.101579>.
- [23] Shamim JA, Hsu W-L, Paul S, Yu L, Daiguiji H. A review of solid desiccant dehumidifiers: current status and near-term development goals in the context of net zero energy buildings. *Renew Sustain Energy Rev* 2021;137:110456. <https://doi.org/10.1016/j.rser.2020.110456>.
- [24] Harriman LG, Plager D, Kosar D. Dehumidification and cooling loads from ventilation air. *Energy Eng J Assoc Energy Eng: Journal of the Association of Energy Engineering* 1999;96:31–45. <https://doi.org/10.1080/01998595.1999.10530479>.
- [25] Son W, Nagai H. Reducing effect of latent heat load by fresh air heat load reduction system using underground double floor space. *J Asian Architect Build Eng* 2004;3:253–8. <https://doi.org/10.3130/jaabe.3.253>.
- [26] Zaki OM, Mohammed RH, Abdelaziz O. Separate sensible and latent cooling technologies: a comprehensive review. *Energy Convers Manag* 2022;256. <https://doi.org/10.1016/j.enconman.2022.115380>.
- [27] Liu X, Jiang Y, Zhang T. Temperature and humidity independent control (THIC) of air-conditioning system 2013;9783642422. <https://doi.org/10.1007/978-3-642-4222-5>.
- [28] Gluesenkamp KR, Nawaz K. Separate sensible and latent cooling: carnot limits and system taxonomy. *Int J Refrig* 2021. <https://doi.org/10.1016/j.ijrefrig.2021.02.019>.
- [29] Miyazaki T, Akisawa A, Saha BB. The performance analysis of a novel dual evaporator type three-bed adsorption chiller. *Int J Refrig* 2010;33:276–85. <https://doi.org/10.1016/j.ijrefrig.2009.10.005>.
- [30] Su W, Zhang X. Thermodynamic analysis of a compression-absorption refrigeration air-conditioning system coupled with liquid desiccant dehumidification. *Appl Therm Eng* 2017;115:575–85. <https://doi.org/10.1016/J.APPLTHERMALENG.2016.12.071>.
- [31] Habib MF, Ali M, Sheikh NA, Badar AW, Mehmood S. Building thermal load management through integration of solar assisted absorption and desiccant air conditioning systems: a model-based simulation-optimization approach. *J Build Eng* 2020;30:101279. <https://doi.org/10.1016/J.JBODE.2020.101279>.
- [32] Luo WJ, Kuo HC, Wu JY, Faridah D. Development and analysis of a new multi-function heat recovery split air conditioner with parallel refrigerant pipe. *Adv Mech Eng* 2016;8:1–12. <https://doi.org/10.1177/1687814016671444>.
- [33] Subramanyam N, Maiya MP, Murthy SS. Application of desiccant wheel to control humidity in air-conditioning systems. *Appl Therm Eng* 2004;24. <https://doi.org/10.1016/j.aplthermaleng.2004.04.008>.
- [34] Peng D, Zhou J, Luo D. Exergy analysis of a liquid desiccant evaporative cooling system. *Int J Refrig* 2017;82:495–508. <https://doi.org/10.1016/j.ijrefrig.2017.06.021>.
- [35] Enteria N, Yoshino H, Takaki R, Yonekura H, Satake A, Mochida A. First and second law analyses of the developed solar-desiccant air-conditioning system (SDACS) operation during the summer day. *Energy Build* 2013;60:239–51. <https://doi.org/10.1016/j.enbuild.2013.01.009>.
- [36] Ath Mohammad, Mat S bin, Sulaiman MY, Sopian K, Al-abidi AA. Survey of liquid desiccant dehumidification system based on integrated vapor compression technology for building applications. *Energy Build* 2013;62. <https://doi.org/10.1016/j.enbuild.2013.03.001>.
- [37] Khosravi S, Yau YH, Mahlia TMI, Saidi MH. A new approach to exergy analyses of a hybrid desiccant cooling system compares to a vapor compression system. *Appl Mech Mater* 2012;110–116:2163–9. <https://doi.org/10.4028/www.scientific.net/AMM.110-116.2163>.
- [38] Jia CX, Dai YJ, Wu JY, Wang RZ. Analysis on a hybrid desiccant air-conditioning system. *Appl Therm Eng* 2006;26:2393–400. <https://doi.org/10.1016/j.aplthermaleng.2006.02.016>.
- [39] Liu W, Lian Z, Radermacher R, Yao Y. Energy consumption analysis on a dedicated outdoor air system with rotary desiccant wheel. *Energy* 2007;32:1749–60. <https://doi.org/10.1016/J.ENERGY.2006.11.012>.
- [40] Hürdoan E, Büyükkalaca O, Yilmaz T, Hepbali A. Experimental investigation of a novel desiccant cooling system. *Energy Build* 2010;42:2049–60. <https://doi.org/10.1016/J.ENBUILD.2010.06.014>.
- [41] Ling J, Kuwabara O, Hwang Y, Radermacher R. Experimental evaluation and performance enhancement prediction of desiccant assisted separate sensible and latent cooling air-conditioning system. *Int J Refrig* 2011;34:946–57. <https://doi.org/10.1016/j.ijrefrig.2010.12.008>.
- [42] Jiang Y, Ge TS, Wang RZ, Huang Y. Experimental investigation on a novel temperature and humidity independent control air conditioning system – Part I: cooling condition. *Appl Therm Eng* 2014;73. <https://doi.org/10.1016/j.aplthermaleng.2014.08.028>.
- [43] Jani DB, Mishra M, Sahoo PK. Performance studies of hybrid solid desiccant-vapor compression air-conditioning system for hot and humid climates. *Energy Build* 2015;102. <https://doi.org/10.1016/j.enbuild.2015.05.055>.
- [44] Jani DB, Mishra M, Sahoo PK. Experimental investigation on solid desiccant-vapor compression hybrid air-conditioning system in hot and humid weather. *Appl Therm Eng* 2016;104. <https://doi.org/10.1016/j.aplthermaleng.2016.05.104>.
- [45] Lee H, Lin X, Hwang Y, Radermacher R. Performance investigation on solid desiccant assisted mobile air conditioning system. *Appl Therm Eng* 2016;103:1370–80. <https://doi.org/10.1016/j.aplthermaleng.2016.05.053>.
- [46] Lee Y, Park S, Kang S. Performance analysis of a solid desiccant cooling system for a residential air conditioning system. *Appl Therm Eng* 2021;182:116091. <https://doi.org/10.1016/J.APPLTHERMALENG.2020.116091>.
- [47] Choi S, Choi S. Desiccant cooling assisted vapor compression system: a double stage desiccant cooling cycle via evaporative condenser. *Appl Therm Eng* 2021;117456. <https://doi.org/10.1016/J.APPLTHERMALENG.2021.117456>.
- [48] Tu YD, Wang RZ, Ge TS, Zheng X. Comfortable, high-efficiency heat pump with desiccant-coated, water-sorbing heat exchangers. *Sci Rep* 2017;7:1–10. <https://doi.org/10.1038/srep40437>.
- [49] Jani DB, Mishra M, Sahoo PK. Performance analysis of a solid desiccant assisted hybrid space cooling system using TRNSYS. *J Build Eng* 2018;19:26–35. <https://doi.org/10.1016/j.jobe.2018.04.016>.

- [50] Worek WM, Khinkis M, Kalensky D, Maisotsenko V. Integrated desiccant–indirect evaporative cooling system utilizing the maisotsenko cycle. Heat transfer in energy systems; theory and fundamental research; aerospace heat transfer; gas turbine heat transfer; transport phenomena in materials processing and manufacturing; heat and, ume 1. ASME; 2012. <https://doi.org/10.1115/HT2012-58039>.
- [51] Zhu J, Chen W. Energy and exergy performance analysis of a marine rotary desiccant air-conditioning system based on orthogonal experiment. *Energy* 2014; 77:953–62. <https://doi.org/10.1016/j.energy.2014.10.014>.
- [52] Pandelidis D, Anisimov S, Worek WM, Drag P. Numerical analysis of a desiccant system with cross-flow Maisotsenko cycle heat and mass exchanger. *Energy Build* 2016;123:136–50. <https://doi.org/10.1016/J.ENBUILD.2016.04.039>.
- [53] Delfani S, Karami M. Transient simulation of solar desiccant/M-Cycle cooling systems in three different climatic conditions. *J Build Eng* 2020;29:101152. <https://doi.org/10.1016/J.JBODE.2019.101152>.
- [54] Chung JD, Lee DY. Contributions of system components and operating conditions to the performance of desiccant cooling systems. *Int J Refrig* 2011;34:922–7. <https://doi.org/10.1016/J.IJREFRIG.2011.03.003>.
- [55] Caliskan H, Lee DY, Hong H. Enhanced thermodynamic assessments of the novel desiccant air cooling system for sustainable energy future. *J Clean Prod* 2019;211: 213–21. <https://doi.org/10.1016/J.JCLEPRO.2018.11.174>.
- [56] Narayanan R, Halawa E, Jain S. Dehumidification potential of a solid desiccant based evaporative cooling system with an enthalpy exchanger operating in subtropical and tropical climates. *Energies* 2019;12:2704. <https://doi.org/10.3390/EN12142704>.
- [57] Beccali M, Finocchiaro P, Nocke B. Energy and economic assessment of desiccant cooling systems coupled with single glazed air and hybrid PV/thermal solar collectors for applications in hot and humid climate. *Sol Energy* 2009;83: 1828–46. <https://doi.org/10.1016/J.SOLENER.2009.06.015>.
- [58] Fong KF, Chow TT, Lee CK, Lin Z, Chan LS. Advancement of solar desiccant cooling system for building use in subtropical Hong Kong. *Energy Build* 2010;42: 2386–99. <https://doi.org/10.1016/J.ENBUILD.2010.08.008>.
- [59] Al-Alili A, Hwang Y, Radermacher R, Kubo I. A high efficiency solar air conditioner using concentrating photovoltaic/thermal collectors. *Appl Energy* 2012;93:138–47. <https://doi.org/10.1016/J.APENERGY.2011.05.010>.
- [60] La D, Dai Y, Li Y, Ge T, Wang R. Case study and theoretical analysis of a solar driven two-stage rotary desiccant cooling system assisted by vapor compression air-conditioning. *Sol Energy* 2011;85:2997–3009. <https://doi.org/10.1016/J.SOLENER.2011.08.039>.
- [61] Angrisani G, Roselli C, Sasso M, Tariello F. Dynamic performance assessment of a solar-assisted desiccant-based air handling unit in two Italian cities. *Energy Convers Manag* 2016;113:331–45. <https://doi.org/10.1016/J.ENCONMAN.2016.01.052>.
- [62] Saghaifar M, Gadalla M. Performance assessment of integrated PV/T and solid desiccant air-conditioning systems for cooling buildings using Maisotsenko cooling cycle. *Sol Energy* 2016;127:79–95. <https://doi.org/10.1016/J.SOLENER.2015.12.048>.
- [63] Qadar Chaudhary G, Ali M, Sheikh NA, Gilani Si ul H, Khushnood S. Integration of solar assisted solid desiccant cooling system with efficient evaporative cooling technique for separate load handling. *Appl Therm Eng* 2018;140:696–706. <https://doi.org/10.1016/j.applthermeng.2018.05.081>.
- [64] Heidari A, Roshandel R, Vakiloroaya V. An innovative solar assisted desiccant-based evaporative cooling system for co-production of water and cooling in hot and humid climates. *Energy Convers Manag* 2019;185:396–409. <https://doi.org/10.1016/J.ENCONMAN.2019.02.015>.
- [65] Rayegan S, Motaghian S, Heidarnejad G, Pasdarshahri H, Ahmadi P, Rosen MA. Dynamic simulation and multi-objective optimization of a solar-assisted desiccant cooling system integrated with ground source renewable energy. *Appl Therm Eng* 2020;173:115210. <https://doi.org/10.1016/J.APPLTHERMALENG.2020.115210>.
- [66] Liu Y, Chen Y, Wang D, Liu J, Li L, Luo X, et al. Performance evaluation of a hybrid solar powered rotary desiccant wheel air conditioning system for low latitude isolated islands. *Energy Build* 2020;224:110208. <https://doi.org/10.1016/J.ENBUILD.2020.110208>.
- [67] Song J, Sobhani B. Energy and exergy performance of an integrated desiccant cooling system with photovoltaic/thermal using phase change material and maisotsenko cooler. *J Energy Storage* 2020;32:101698. <https://doi.org/10.1016/J.JEST.2020.101698>.
- [68] Saedpanah E, Pasdarshahri H. Performance assessment of hybrid desiccant air conditioning systems: a dynamic approach towards achieving optimum 3E solution across the lifespan. *Energy* 2021;234:121151. <https://doi.org/10.1016/J.ENERGY.2021.121151>.
- [69] Li H, Dai YJ, Li Y, La D, Wang RZ. Experimental investigation on a one-rotor two-stage desiccant cooling/heating system driven by solar air collectors. *Appl Therm Eng* 2011;31:3677–83. <https://doi.org/10.1016/J.APPLTHERMALENG.2011.01.018>.
- [70] Zeng DQ, Li H, Dai YJ, Xie AX. Numerical analysis and optimization of a solar hybrid one-rotor two-stage desiccant cooling and heating system. *Appl Therm Eng* 2014;73:474–83. <https://doi.org/10.1016/J.APPLTHERMALENG.2014.07.076>.
- [71] Kousar R, Ali M, Sheikh NA, Gilani Si ul H, Khushnood S. Holistic integration of multi-stage dew point counter flow indirect evaporative cooler with the solar-assisted desiccant cooling system: a techno-economic evaluation. *Energy for Sustainable Development* 2021;62:163–74. <https://doi.org/10.1016/J.ESD.2021.04.005>.
- [72] Zhou X. Thermal and energy performance of a solar-driven desiccant cooling system using an internally cooled desiccant wheel in various climate conditions. *Appl Therm Eng* 2021;185:116077. <https://doi.org/10.1016/J.APPLTHERMALENG.2020.116077>.
- [73] Ling J, Kuwabara O, Hwang Y, Radermacher R. Enhancement options for separate sensible and latent cooling air-conditioning systems. *Int J Refrig* 2013;36:45–57. <https://doi.org/10.1016/J.IJREFRIG.2012.09.003>.
- [74] Sheng Y, Zhang H, Deng N, Fang L, Nie J, Ma L. Experimental analysis on performance of high temperature heat pump and desiccant wheel system. *Energy Build* 2013;66. <https://doi.org/10.1016/j.enbuild.2013.07.058>.
- [75] Luo WJ, Faridah D, Fasya FR, Chen YS, Mulki FH, Adilah UN. Performance enhancement of hybrid solid desiccant cooling systems by integrating solar water collectors in Taiwan. *Energies* 2019;12:1–18. <https://doi.org/10.3390/en12183470>.
- [76] Nie J, Li Z, Hu W, Fang L, Zhang Q. Theoretical modelling and experimental study of air thermal conditioning process of a heat pump assisted solid desiccant cooling system. *Energy Build* 2017;153:31–40. <https://doi.org/10.1016/J.ENBUILD.2017.07.075>.
- [77] Mohammad AT, Mat S bin, Sulaiman MY, Sopian K, Al-Abidi AA. Survey of liquid desiccant dehumidification system based on integrated vapor compression technology for building applications. *Energy Build* 2013;62:1–14. <https://doi.org/10.1016/J.ENBUILD.2013.03.001>.
- [78] Studak JW, Peterson JL. A preliminary evaluation of alternative liquid desiccants for a hybrid desiccant air conditioner. 1988.
- [79] Kinsara AA, Elsayed MM, Al-Rabghi OM. Proposed energy-efficient air-conditioning system using liquid desiccant. *Appl Therm Eng* 1996;16:791–806. [https://doi.org/10.1016/1359-4311\(95\)00090-9](https://doi.org/10.1016/1359-4311(95)00090-9).
- [80] Dai YJ, Wang RZ, Zhang HF, Yu JD. Use of liquid desiccant cooling to improve the performance of vapor compression air conditioning. *Appl Therm Eng* 2001;21. [https://doi.org/10.1016/S1359-4311\(01\)00002-3](https://doi.org/10.1016/S1359-4311(01)00002-3).
- [81] Chen Z, Zhu J, Bai H, Yan Y, Zhang L. Experimental study of a membrane-based dehumidification cooling system. *Appl Therm Eng* 2017;115:1315–21. <https://doi.org/10.1016/J.APPLTHERMALENG.2016.10.153>.
- [82] Mansuriya K, Raja BD, Patel VK. Experimental assessment of a small scale hybrid liquid desiccant dehumidification incorporated vapor compression refrigeration system: an energy saving approach. *Appl Therm Eng* 2020;174:115288. <https://doi.org/10.1016/J.APPLTHERMALENG.2020.115288>.
- [83] Mansuriya K, Patel VK, Raja BD, Mudgal A. Assessment of liquid desiccant dehumidification aided vapor-compression refrigeration system based on thermo-economic approach. *Appl Therm Eng* 2020;164:114542. <https://doi.org/10.1016/J.APPLTHERMALENG.2019.114542>.
- [84] Khalil A. An experimental study on multi-purpose desiccant integrated vapor-compression air-conditioning system. *JES Journal of Engineering Sciences* 2010; 38:105–18. <https://doi.org/10.21608/jesaua.2010.123785>.
- [85] Zhao K, Liu XH, Zhang T, Jiang Y. Performance of temperature and humidity independent control air-conditioning system in an office building. *Energy Build* 2011;43:1895–903. <https://doi.org/10.1016/J.ENBUILD.2011.03.041>.
- [86] Bergero S, Chiari A. Performance analysis of a liquid desiccant and membrane contactor hybrid air-conditioning system. *Energy Build* 2010;42:1976. <https://doi.org/10.1016/J.ENBUILD.2010.06.003>–86.
- [87] Bergero S, Chiari A. On the performances of a hybrid air-conditioning system in different climatic conditions. *Energy* 2011;36:5261–73. <https://doi.org/10.1016/J.ENERGY.2011.06.030>.
- [88] Zhang L, Hihara E, Saikawa M. Combination of air-source heat pumps with liquid desiccant dehumidification of air. *Energy Convers Manag* 2012;57:107–16. <https://doi.org/10.1016/J.ENCONMAN.2011.12.023>.
- [89] Zhang L, Dang C, Hihara E. Performance analysis of a no-frost hybrid air conditioning system with integrated liquid desiccant dehumidification. *Int J Refrig* 2010;33:116–24. <https://doi.org/10.1016/J.IJREFRIG.2009.08.007>.
- [90] Lee JH, Jeong JW. Hybrid heat-pump-driven liquid-desiccant system: experimental performance analysis for residential air-conditioning applications. *Appl Therm Eng* 2021;195:117236. <https://doi.org/10.1016/J.APPLTHERMALENG.2021.117236>.
- [91] Yamaguchi S, Jeong J, Saito K, Miyauchi H, Harada M. Hybrid liquid desiccant air-conditioning system: experiments and simulations. *Appl Therm Eng* 2011;31: 3741–7. <https://doi.org/10.1016/J.APPLTHERMALENG.2011.04.009>.
- [92] Xie Y, Zhang T, Liu X. Performance investigation of a counter-flow heat pump driven liquid desiccant dehumidification system. *Energy* 2016;115:446–57. <https://doi.org/10.1016/J.ENERGY.2016.09.037>.
- [93] Liu J, Zhang T, Liu X. Model-based investigation of a heat pump driven, internally cooled liquid desiccant dehumidification system. *Build Environ* 2018;143: 431–42. <https://doi.org/10.1016/J.BUILDENV.2018.07.027>.
- [94] Li Z, Liu X, Jiang Y, Chen X. New type of fresh air processor with liquid desiccant total heat recovery. *Energy Build* 2005;37. <https://doi.org/10.1016/j.enbuild.2004.09.017>.
- [95] He H, Wang L, Yuan J, Wang Z, Fu W, Liang K. Performance evaluation of solar absorption-compression cascade refrigeration system with an integrated air-cooled compression cycle. *Energy Convers Manag* 2019;201:112153. <https://doi.org/10.1016/J.ENCONMAN.2019.112153>.
- [96] Guan B, Liu X, Zhang T, Liu J. Optimal flow type in internally-cooled liquid-desiccant system driven by heat pump: component level vs. System level. *Appl Therm Eng* 2021;183:116208. <https://doi.org/10.1016/J.APPLTHERMALENG.2020.116208>.
- [97] Guan B, Liu X, Zhang Q, Zhang T. Performance of a temperature and humidity independent control air-conditioning system based on liquid desiccant for

- industrial environments. *Energy Build* 2020;214. <https://doi.org/10.1016/j.enbuild.2020.109869>.
- [98] Song M, Wang L, Yuan J, Wang Z, Li X, Liang K. Proposal and parametric study of solar absorption/dual compression hybrid refrigeration system for temperature and humidity independent control application. *Energy Convers Manag* 2020;220. <https://doi.org/10.1016/j.enconman.2020.113107>.
- [99] Ali M, Habib MF, Ahmed Sheikh N, Akhter J, Gilani Si ul H. Experimental investigation of an integrated absorption- solid desiccant air conditioning system. *Appl Therm Eng* 2022;203:117912. <https://doi.org/10.1016/J.APPLTHERMALENG.2021.117912>.
- [100] Yong L, Sumathy K, Dai YJ, Zhong JH, Wang RZ. Experimental study on a hybrid desiccant dehumidification and air conditioning system. *Journal of Solar Energy Engineering, Transactions of the ASME* 2006;128:77–82. <https://doi.org/10.1115/1.2148977>.
- [101] Abdel-Salam AH, Ge G, Simonson CJ. Thermo-economic performance of a solar membrane liquid desiccant air conditioning system. *Sol Energy* 2014;102:56–73. <https://doi.org/10.1016/J.SOLENER.2013.12.036>.
- [102] Ma Q, Wang RZ, Dai YJ, Zhai XQ. Performance analysis on a hybrid air-conditioning system of a green building. *Energy Build* 2006;38:447–53. <https://doi.org/10.1016/J.ENBUILD.2005.08.004>.
- [103] Mujahid Rafique M, Gandhisadas P, Rehman S, Al-Hadrami LM. A review on desiccant based evaporative cooling systems. *Renew Sustain Energy Rev* 2015;45: 145–59. <https://doi.org/10.1016/j.rser.2015.01.051>.
- [104] Buker MS, Riffat SB. Recent developments in solar assisted liquid desiccant evaporative cooling technology—a review. *Energy Build* 2015;96:95–108. <https://doi.org/10.1016/j.enbuild.2015.03.020>.
- [105] Kim M-H, Park J-S, Jeong J-W. Energy saving potential of liquid desiccant in evaporative-cooling-assisted 100% outdoor air system. *Energy* 2013;59:726–36. <https://doi.org/10.1016/j.energy.2013.07.018>.
- [106] Lee S-J, Kim H-J, Dong H-W, Jeong J-W. Energy saving assessment of a desiccant-enhanced evaporative cooling system in variable air volume applications. *Appl Therm Eng* 2017;117:94–108. <https://doi.org/10.1016/j.aplthermaleng.2017.02.007>.
- [107] Zhang F, Yin Y, Zhang X. Performance analysis of a novel liquid desiccant evaporative cooling fresh air conditioning system with solution recirculation. *Build Environ* 2017;117:218–29. <https://doi.org/10.1016/j.buildenv.2017.03.015>.
- [108] U.S. Energy Information Administration. Form EIA-860 annual electric generator report. 2019.
- [109] Fauchoux MT, Simonson CJ, Torvi DA. Investigation of a novel ceiling panel for heat and moisture control in buildings, vol. 62. Copenhagen, Denmark: 8th Nordic Symposium on Buildings Physics; 2008. p. 1269–76.
- [110] Eldeeb R, Fauchoux M, Simonson CJ. Applicability of a heat and moisture transfer panel (HAMP) for maintaining space relative humidity in an office building using TRNSYS. *Energy Build* 2013;66:338–45. <https://doi.org/10.1016/j.enbuild.2013.07.021>.
- [111] Keniar K, Ghali K, Ghaddar N. Study of solar regenerated membrane desiccant system to control humidity and decrease energy consumption in office spaces. *Appl Energy* 2015;138:121–32. <https://doi.org/10.1016/j.apenergy.2014.10.071>.
- [112] Yang W, Deng H, Wang Z, Zhao X, He S. Performance investigation of the novel solar-powered dehumidification window for residential buildings. *Energies* 2017; 10. <https://doi.org/10.3390/en10091369>.
- [113] Zhang Y, Wu L, Wang X, Yu J, Ding B. Super hygroscopic nanofibrous membrane-based moisture pump for solar-driven indoor dehumidification. *Nat Commun* 2020;11:3302. <https://doi.org/10.1038/s41467-020-17118-3>.
- [114] Nandakumar DK, Ravi SK, Zhang Y, Guo N, Zhang C, Tan SC. A super hygroscopic hydrogel for harnessing ambient humidity for energy conservation and harvesting. *Energy Environ Sci* 2018;11:2179–87. <https://doi.org/10.1039/c8ee00902c>.
- [115] Imanari T, Omori T, Bogaki K. Thermal comfort and energy consumption of the radiant ceiling panel system. *Energy Build* 1999;30:167–75. [https://doi.org/10.1016/s0378-7788\(98\)00084-x](https://doi.org/10.1016/s0378-7788(98)00084-x).
- [116] Vangtook P, Chirarattananon S. An experimental investigation of application of radiant cooling in hot humid climate. *Energy Build* 2006;38:273–85. <https://doi.org/10.1016/j.enbuild.2005.06.022>.
- [117] Kim T, Kato S, Murakami S, Rho JW. Study on indoor thermal environment of office space controlled by cooling panel system using field measurement and the numerical simulation. *Build Environ* 2005;40:301–10. <https://doi.org/10.1016/j.buildenv.2004.04.010>.
- [118] Fauchoux MT, Simonson CJ, Torvi DA. Investigation of a novel ceiling panel for heat and moisture control in buildings, vol. 62. Copenhagen, Denmark: 8th Nordic Symposium on Buildings Physics; 2008. p. 1269–76.
- [119] Eldeeb R, Fauchoux M, Simonson CJ. Applicability of a heat and moisture transfer panel (HAMP) for maintaining space relative humidity in an office building using TRNSYS. *Energy Build* 2013;66:338–45. <https://doi.org/10.1016/j.enbuild.2013.07.021>.
- [120] Keniar K, Ghali K, Ghaddar N. Study of solar regenerated membrane desiccant system to control humidity and decrease energy consumption in office spaces. *Appl Energy* 2015;138:121–32. <https://doi.org/10.1016/j.apenergy.2014.10.071>.
- [121] Yang W, Deng H, Wang Z, Zhao X, He S. Performance investigation of the novel solar-powered dehumidification window for residential buildings. *Energies* 2017; 10. <https://doi.org/10.3390/en10091369>.
- [122] Rezaei SD, Shannigrahi S, Ramakrishna S. A review of conventional, advanced, and smart glazing technologies and materials for improving indoor environment. *Sol Energy Mater Sol Cell* 2017;159:26–51. <https://doi.org/10.1016/j.solmat.2016.08.026>.
- [123] Aburas M, Soebarto V, Williamson T, Liang R, Ebendorff-Heidepriem H, Wu Y. Thermochromic smart window technologies for building application: a review. *Appl Energy* 2019;255:113522. <https://doi.org/10.1016/j.apenergy.2019.113522>.
- [124] Zhou Y, Dong X, Mi Y, Fan F, Xu Q, Zhao H, et al. Hydrogel smart windows. *J Mater Chem A Mater* 2020;8:10007–25. <https://doi.org/10.1039/d0ta00849d>.
- [125] Zhou Y, Fan F, Liu Y, Zhao S, Xu Q, Wang S, et al. Unconventional smart windows: materials, structures and designs. *Nano Energy* 2021;90:106613. <https://doi.org/10.1016/j.nanoen.2021.106613>.
- [126] Nandakumar DK, Ravi SK, Zhang Y, Guo N, Zhang C, Tan SC. A super hygroscopic hydrogel for harnessing ambient humidity for energy conservation and harvesting. *Energy Environ Sci* 2018;11:2179–87. <https://doi.org/10.1039/c8ee00902c>.
- [127] Li B, Hua L, Tu Y, Wang R. A full-solid-state humidity pump for localized humidity control. *Joule* 2019;3:1427–36. <https://doi.org/10.1016/j.joule.2019.03.018>.
- [128] Hou P, Zu K, Qin M, Cui S. A novel metal-organic frameworks based humidity pump for indoor moisture control. *Build Environ* 2021;187:107396. <https://doi.org/10.1016/j.buildenv.2020.107396>.
- [129] Kessling W, Laevemann E, Peltzer M. Energy storage in open cycle liquid desiccant cooling systems. *Int J Refrig* 1998;21:150–6. [https://doi.org/10.1016/S0140-7007\(97\)00045-5](https://doi.org/10.1016/S0140-7007(97)00045-5).
- [130] Zhu D, Wu H, Wang S. Experimental study on composite silica gel supported CaCl₂ sorbent for low grade heat storage. *Int J Therm Sci* 2006;45:804–13. <https://doi.org/10.1016/j.ijthermalsci.2005.10.009>.
- [131] Hongois S, Kuznik F, Stevens P, Roux JJ. Development and characterisation of a new MgSO₄-zeolite composite for long-term thermal energy storage. *Sol Energy Mater Sol Cell* 2011;95:1831–7. <https://doi.org/10.1016/j.solmat.2011.01.050>.
- [132] Solé A, Martorell I, Cabeza LF. State of the art on gas-solid thermochemical energy storage systems and reactors for building applications. *Renew Sustain Energy Rev* 2015;47:386–98. <https://doi.org/10.1016/j.rser.2015.03.077>.
- [133] Frazzica A, Freni A. Adsorbent working pairs for solar thermal energy storage in buildings. *Renew Energy* 2017;110:87–94. <https://doi.org/10.1016/j.renene.2016.09.047>.
- [134] Zhang Y, Wang R. Sorption thermal energy storage: concept, process, applications and perspectives. *Energy Storage Mater* 2020;27:352–69. <https://doi.org/10.1016/j.ensm.2020.02.024>.
- [135] Riaz F, Qayum MA, Bokhari A, Klemeš JJ, Usman M, Asim M, et al. Design and energy analysis of a solar desiccant evaporative cooling system with built-in daily energy storage. *Energies* 2021;14. <https://doi.org/10.3390/en14092429>.
- [136] Wang Z, Li R, Yin F, Wu Y, Gu Z. Experimentation of a membrane-based concentration gradient energy storage of liquid desiccant solutions driven by solar energy. *J Therm Sci* 2021;30:1503–12. <https://doi.org/10.1007/s11630-021-1411-x>.
- [137] Rady MA. Experimental and numerical investigations on the performance of dehumidifying desiccant beds composed of silica-gel and thermal energy storage particles. *Heat and Mass Transfer/Waerme- Und Stoffuebertragung* 2009;45: 545–61. <https://doi.org/10.1007/s00231-008-0459-4>.
- [138] Li W, Luo X, Yang P, Wang Q, Zeng M, Markides CN. Solar-thermal energy conversion prediction of building envelope using thermochemical sorbent based on established reaction kinetics. *Energy Convers Manag* 2022;252:115117. <https://doi.org/10.1016/j.enconman.2021.115117>.
- [139] Kuznik F, Johannes K, Obrecht C, David D. A review on recent developments in physisorption thermal energy storage for building applications. *Renew Sustain Energy Rev* 2018;94:576–86. <https://doi.org/10.1016/j.rser.2018.06.038>.
- [140] Shigeishi RA, Langford CH, Holbone BR. Solar energy storage using chemical potential changes associated with drying of zeolites. *Sol Energy* 1979;23:489–95. [https://doi.org/10.1016/0038-092X\(79\)90072-0](https://doi.org/10.1016/0038-092X(79)90072-0).
- [141] Jänenchen J, Stach H. Adsorption properties of porous materials for solar thermal energy storage and heat pump applications. *Energy Proc* 2012;30:289–93. <https://doi.org/10.1016/j.egypro.2012.11.034>.
- [142] Hauer A. Thermal energy storage with zeolite for heating and cooling applications. *International Sorption Heat Pump Conference 2002* 2002;1:385–90.
- [143] Kabeel AE, Khalil A, Elsayed SS, Alatyar AM. Theoretical investigation on energy storage characteristics of a solar liquid desiccant air conditioning system in Egypt. *Energy* 2018;158:164–80. <https://doi.org/10.1016/j.energy.2018.06.014>.
- [144] Palomba V, Frazzica A. Recent advancements in sorption technology for solar thermal energy storage applications. *Sol Energy* 2019;192:69–105. <https://doi.org/10.1016/j.solener.2018.06.102>.
- [145] Liu XH, Geng KC, Lin BR, Jiang Y. Combined cogeneration and liquid-desiccant system applied in a demonstration building. *Energy Build* 2004;36:945–53. <https://doi.org/10.1016/j.enbuild.2004.03.001>.
- [146] Lävemann E, Peltzer M, Hublitz a, Kroenauer a, Raab U, Hauer a. *Thermochemical storage for air-conditioning using open cycle liquid desiccant technology*. Pomona, NJ: Stockton College of New Jersey; 2006.
- [147] Solé A, Martorell I, Cabeza LF. State of the art on gas-solid thermochemical energy storage systems and reactors for building applications. *Renew Sustain Energy Rev* 2015;47:386–98. <https://doi.org/10.1016/j.rser.2015.03.077>.
- [148] Frazzica A, Freni A. Adsorbent working pairs for solar thermal energy storage in buildings. *Renew Energy* 2017;110:87–94. <https://doi.org/10.1016/j.renene.2016.09.047>.
- [149] Johannes K, Kuznik F, Hubert JL, Durier F, Obrecht C. Design and characterisation of a high powered energy dense zeolite thermal energy storage

- system for buildings. *Appl Energy* 2015;159:80–6. <https://doi.org/10.1016/j.apenergy.2015.08.109>.
- [150] Zhu D, Wu H, Wang S. Experimental study on composite silica gel supported CaCl₂ sorbent for low grade heat storage. *Int J Therm Sci* 2006;45:804–13. <https://doi.org/10.1016/j.ijthermalsci.2005.10.009>.
- [151] Wang Z, Li R, Yin F, Wu Y, Gu Z. Experimentation of a membrane-based concentration gradient energy storage of liquid desiccant solutions driven by solar energy. *J Therm Sci* 2021;30:1503–12. <https://doi.org/10.1007/s11630-021-1411-x>.
- [152] Kabeel AE, Khalil A, Elsayed SS, Alatyar AM. Theoretical investigation on energy storage characteristics of a solar liquid desiccant air conditioning system in Egypt. *Energy* 2018;158:164–80. <https://doi.org/10.1016/j.energy.2018.06.014>.
- [153] Palomba V, Frazzica A. Recent advancements in sorption technology for solar thermal energy storage applications. *Sol Energy* 2019;192:69–105. <https://doi.org/10.1016/j.solener.2018.06.102>.
- [154] Kuznik F, Johannes K, Obrecht C, David D. A review on recent developments in physisorption thermal energy storage for building applications. *Renew Sustain Energy Rev* 2018;94:576–86. <https://doi.org/10.1016/j.rser.2018.06.038>.
- [155] Finck C, Henquet E, Van Soest C, Oversloot H, De Jong AJ, Cuypers R, et al. Experimental results of a 3 kWh thermochemical heat storage module for space heating application. *Energy Proc* 2014;48:320–6. <https://doi.org/10.1016/j.egypro.2014.02.037>.
- [156] Köll R, van Helden W, Engel G, Wagner W, Dang B, Jänenchen J, et al. An experimental investigation of a realistic-scale seasonal solar adsorption storage system for buildings. *Sol Energy* 2017;155:388–97. <https://doi.org/10.1016/j.solener.2017.06.043>.
- [157] Li TX, Wu S, Yan T, Wang RZ, Zhu J. Experimental investigation on a dual-mode thermochemical sorption energy storage system. *Energy* 2017;140:383–94. <https://doi.org/10.1016/j.energy.2017.08.073>.
- [158] Kant K, Shukla A, Smeulders DMJ, Rindt CCM. Analysis and optimization of the closed-adsorption heat storage bed performance. *J Energy Storage* 2020;32: 101896. <https://doi.org/10.1016/j.est.2020.101896>.
- [159] Popah-Lele A, Rohde C, Neumann K, Tietjen T, Rönnebeck T, N'Tsoukpo KE, et al. Lab-scale experiment of a closed thermochemical heat storage system including honeycomb heat exchanger. *Energy* 2016;114:225–38. <https://doi.org/10.1016/j.energy.2016.08.009>.
- [160] Xu SZ, Lemington Wang RZ, Wang LW, Zhu J. A zeolite 13X/magnesium sulfate–water sorption thermal energy storage device for domestic heating. *Energy Convers Manag* 2018;171:98–109. <https://doi.org/10.1016/j.enconman.2018.05.077>.
- [161] Ehrenmann J, Henninger SK, Janiak C. Water adsorption characteristics of MIL-101 for heat-transformation applications of MOFs. 2011. p. 471–4.
- [162] Xu SZ, Lemington Wang RZ, Wang LW, Zhu J. A zeolite 13X/magnesium sulfate–water sorption thermal energy storage device for domestic heating. *Energy Convers Manag* 2018;171:98–109. <https://doi.org/10.1016/j.enconman.2018.05.077>.
- [163] Frazzica A, Brancato V, Capri A, Cannilla C, Gordeeva LG, Aristov YI. Development of “salt in porous matrix” composites based on LiCl for sorption thermal energy storage. *Energy* 2020;208:118338. <https://doi.org/10.1016/j.energy.2020.118338>.
- [164] Pryor TL, Close DJ. The behaviour of adsorbent energy storage beds. *Sol Energy* 1978;20:151–5. [https://doi.org/10.1016/0038-092X\(78\)90188-3](https://doi.org/10.1016/0038-092X(78)90188-3).
- [165] Sheridan NR. Performance of the Brisbane Solar House 1972;13:395–401.
- [166] Johannes K, Kuznik F, Hubert JL, Durier F, Obrecht C. Design and characterisation of a high powered energy dense zeolite thermal energy storage system for buildings. *Appl Energy* 2015;159:80–6. <https://doi.org/10.1016/j.apenergy.2015.08.109>.
- [167] Zhang YN, Wang RZ, Li TX. Experimental investigation on an open sorption thermal storage system for space heating. *Energy* 2017;141:2421–33. <https://doi.org/10.1016/j.energy.2017.12.003>.
- [168] Liu H, Nagano K, Togawa J. A composite material made of mesoporous siliceous shale impregnated with lithium chloride for an open sorption thermal energy storage system. *Sol Energy* 2015;111:186–200. <https://doi.org/10.1016/j.solener.2014.10.044>.
- [169] Li W, Guo H, Zeng M, Wang Q. Performance of SrBr₂-H₂O based seasonal thermochemical heat storage in a novel multilayered sieve reactor. *Energy Convers Manag* 2019;198:111843. <https://doi.org/10.1016/j.enconman.2019.111843>.
- [170] Zettl B, Englmair G, Steinmauer G. Development of a revolving drum reactor for open-sorption heat storage processes. *Appl Therm Eng* 2014;70:42–9. <https://doi.org/10.1016/j.applthermaleng.2014.04.069>.
- [171] Farcot L, Le Pierrès N, Fournigüé JF. Experimental investigation of a moving-bed heat storage thermochemical reactor with SrBr₂/H₂O couple. *J Energy Storage* 2019;26:101009. <https://doi.org/10.1016/j.est.2019.101009>.
- [172] Rogala Z, Kolasiński P, Gnutek Z. Modelling and experimental analyzes on air-fluidised silica gel-water adsorption and desorption. *Appl Therm Eng* 2017;127: 950–62. <https://doi.org/10.1016/j.applthermaleng.2017.07.122>.
- [173] Weber R, Dorez V. Long-term heat storage with NaOH. *Vacuum* 2008;82:708–16. <https://doi.org/10.1016/j.vacuum.2007.10.018>.
- [174] Quinnell JA, Davidson JH. Mass transfer during sensible charging of a hybrid absorption/sensible storage tank. *Energy Proc* 2012;30:353–61. <https://doi.org/10.1016/j.egypro.2012.11.042>.
- [175] Zhang X, Li M, Shi W, Wang B, Li X. Experimental investigation on charging and discharging performance of absorption thermal energy storage system. *Energy Convers Manag* 2014;85:425–34. <https://doi.org/10.1016/j.enconman.2014.05.100>.
- [176] Zhao YJ, Wang RZ, Li TX, Nomura Y. Investigation of a 10 kWh sorption heat storage device for effective utilization of low-grade thermal energy. *Energy* 2016; 113:739–47. <https://doi.org/10.1016/j.energy.2016.07.100>.
- [177] N'Tsoukpo KE, Le Pierrès N, Luo L. Experimentalization of a LiBr-H₂O absorption process for long-term solar thermal storage: prototype design and first results. *Energy* 2013;53:179–98. <https://doi.org/10.1016/j.energy.2013.02.023>.
- [178] Le Pierrès N, Huaylla F, Stutz B, Perraud J. Long-term solar heat storage process by absorption with the KCOOH/H₂O couple: experimental investigation. *Energy* 2017;141:1313–23. <https://doi.org/10.1016/j.energy.2017.10.111>.
- [179] N'Tsoukpo KE, Le Pierrès N, Luo L. Experimentation of a LiBr-H₂O absorption process for long-term solar thermal storage: prototype design and first results. *Energy* 2013;53:179–98. <https://doi.org/10.1016/j.energy.2013.02.023>.
- [180] Xu ZY, Wang RZ. Absorption seasonal thermal storage cycle with high energy storage density through multi-stage output. *Energy* 2019;167:1086–96. <https://doi.org/10.1016/j.energy.2018.11.072>.
- [181] Wu W. Low-temperature compression-assisted absorption thermal energy storage using ionic liquids. *Energy and Built Environment* 2020;1:139–48. <https://doi.org/10.1016/j.enbenv.2019.11.001>.
- [182] Finch C, Henquet E, Van Soest C, Oversloot H, De Jong AJ, Cuypers R, et al. Experimental results of a 3 kWh thermochemical heat storage module for space heating application. *Energy Proc* 2014;48:320–6. <https://doi.org/10.1016/j.egypro.2014.02.037>.
- [183] Köll R, van Helden W, Engel G, Wagner W, Dang B, Jänenchen J, et al. An experimental investigation of a realistic-scale seasonal solar adsorption storage system for buildings. *Sol Energy* 2017;155:388–97. <https://doi.org/10.1016/j.solener.2017.06.043>.
- [184] Li TX, Wu S, Yan T, Wang RZ, Zhu J. Experimental investigation on a dual-mode thermochemical sorption energy storage system. *Energy* 2017;140:383–94. <https://doi.org/10.1016/j.energy.2017.08.073>.
- [185] Kant K, Shukla A, Smeulders DMJ, Rindt CCM. Analysis and optimization of the closed-adsorption heat storage bed performance. *J Energy Storage* 2020;32: 101896. <https://doi.org/10.1016/j.est.2020.101896>.
- [186] Popah-Lele A, Rohde C, Neumann K, Tietjen T, Rönnebeck T, N'Tsoukpo KE, et al. Lab-scale experiment of a closed thermochemical heat storage system including honeycomb heat exchanger. *Energy* 2016;114:225–38. <https://doi.org/10.1016/j.energy.2016.08.009>.
- [187] Ehrenmann J, Henninger SK, Janiak C. Water adsorption characteristics of MIL-101 for heat-transformation applications of MOFs. 2011. p. 471–4.
- [188] Frazzica A, Brancato V, Capri A, Cannilla C, Gordeeva LG, Aristov YI. Development of “salt in porous matrix” composites based on LiCl for sorption thermal energy storage. *Energy* 2020;208:118338. <https://doi.org/10.1016/j.energy.2020.118338>.
- [189] Zhang YN, Wang RZ, Li TX. Experimental investigation on an open sorption thermal storage system for space heating. *Energy* 2017;141:2421–33. <https://doi.org/10.1016/j.energy.2017.12.003>.
- [190] Liu H, Nagano K, Togawa J. A composite material made of mesoporous siliceous shale impregnated with lithium chloride for an open sorption thermal energy storage system. *Sol Energy* 2015;111:186–200. <https://doi.org/10.1016/j.solener.2014.10.044>.
- [191] Zettl B, Englmair G, Steinmauer G. Development of a revolving drum reactor for open-sorption heat storage processes. *Appl Therm Eng* 2014;70:42–9. <https://doi.org/10.1016/j.applthermaleng.2014.04.069>.
- [192] Farcot L, Le Pierrès N, Fournigüé JF. Experimental investigation of a moving-bed heat storage thermochemical reactor with SrBr₂/H₂O couple. *J Energy Storage* 2019;26:101009. <https://doi.org/10.1016/j.est.2019.101009>.
- [193] Rogala Z, Kolasiński P, Gnutek Z. Modelling and experimental analyzes on air-fluidised silica gel-water adsorption and desorption. *Appl Therm Eng* 2017;127: 950–62. <https://doi.org/10.1016/j.applthermaleng.2017.07.122>.
- [194] Li W, Guo H, Zeng M, Wang Q. Performance of SrBr₂-H₂O based seasonal thermochemical heat storage in a novel multilayered sieve reactor. *Energy Convers Manag* 2019;198:111843. <https://doi.org/10.1016/j.enconman.2019.111843>.
- [195] Zhao YJ, Wang RZ, Li TX, Nomura Y. Investigation of a 10 kWh sorption heat storage device for effective utilization of low-grade thermal energy. *Energy* 2016; 113:739–47. <https://doi.org/10.1016/j.energy.2016.07.100>.
- [196] Le Pierrès N, Huaylla F, Stutz B, Perraud J. Long-term solar heat storage process by absorption with the KCOOH/H₂O couple: experimental investigation. *Energy* 2017;141:1313–23. <https://doi.org/10.1016/j.energy.2017.10.111>.
- [197] Wu W. Low-temperature compression-assisted absorption thermal energy storage using ionic liquids. *Energy and Built Environment* 2020;1:139–48. <https://doi.org/10.1016/j.enbenv.2019.11.001>.
- [198] Cranston J, Askalany A, Santori G. Efficient drying in washer dryers by combining sorption and heat pumping. *Energy* 2019;183:683–92. <https://doi.org/10.1016/j.energy.2019.06.141>.
- [199] Ahmadi M, Gluesenkamp KR, Bigham S. Energy-efficient sorption-based gas clothes dryer systems. *Energy Convers Manag* 2021;230:113763. <https://doi.org/10.1016/j.enconman.2020.113763>.
- [200] El Fil B, Garimella S. Energy-efficient gas-fired tumble dryer with adsorption thermal storage. *Energy* 2022;239. <https://doi.org/10.1016/j.energy.2021.121708>.
- [201] El Fil B, Garimella S. Waste heat recovery in commercial gas-fired tumble dryers. *Energy* 2021;218:119407. <https://doi.org/10.1016/j.energy.2020.119407>.
- [202] Cranston J, Askalany A, Santori G. Efficient drying in washer dryers by combining sorption and heat pumping. *Energy* 2019;183:683–92. <https://doi.org/10.1016/j.energy.2019.06.141>.

- [203] El Fil B, Garimella S. Heat recovery, adsorption thermal storage, and heat pumping to augment gas-fired tumble dryer efficiency. *J Energy Storage* 2022;48: 103949. <https://doi.org/10.1016/j.est.2021.103949>.
- [204] Hauer A, Fischer F. Open adsorption system for an energy efficient dishwasher. *Chem Ing Tech* 2011;83:61–6. <https://doi.org/10.1002/cite.201000197>.
- [205] Santori G, Frazzica A, Freni A, Galieni M, Bonaccorsi L, Polonara F, et al. Optimization and testing on an adsorption dishwasher. *Energy* 2013;50:170–6. <https://doi.org/10.1016/j.energy.2012.11.031>.
- [206] Hauer A, Fischer F. Open adsorption system for an energy efficient dishwasher. *Chem Ing Tech* 2011;83:61–6. <https://doi.org/10.1002/cite.201000197>.